AD-769 930

AN EXPERIMENTAL STUDY OF ATTENUATION OF SHOCK WAVES IN AIRCRAFT FUEL TANKS

John R. Breuninger, Jr.

Air Force Institute of Technology
Wright-Patterson Air Force Base, Ohio

June 1973

AD769930

DOCUMENT CONTROL DATA - R & D

(Security classification of title, body of abstract and indexing annotation must be entered when the overall report is classified)

1. ORIGINATING ACTIVITY (Corporate author)
Air Institute of Technology (AU)
Wright-Patterson AFB, Ohio

2a. REPORT SECURITY CLASSIFICATION
UNCLASSIFIED

2b. GROUP

3. REPORT TITLE
An Experimental Study of Attenuation of Shock Waves in Aircraft Fuel Tanks

4. DESCRIPTIVE NOTES (Type of report and inclusive dates)
Thesis

5. AUTHOR(S) (First name, middle initial, last name)
John R. Breuninger, Jr.
Capt USAF

6. REPORT DATE
June 1973

7a. TOTAL NO. OF PAGES
73

7b. NO. OF REFS
11

8a. CONTRACT OR GRANT NO.

b. PROJECT NO.

c.

d.

9a. ORIGINATOR'S REPORT NUMBER(S)
GA/MC/73-3

9b. OTHER REPORT NO(S) (Any other numbers that may be assigned this report)

10. DISTRIBUTION STATEMENT
Approved for public release; distribution unlimited.

Approved for public release; IAW AFR 190-17
JERRY C. HIX, Captain, USAF
Director of Information

11. SUPPLEMENTARY NOTES

12. SPONSORING MILITARY ACTIVITY
AF Flight Dynamics Laboratory
Wright-Patterson Air Force Base, Ohio

13. ABSTRACT

When a full, or partially full, aircraft fuel tank is penetrated by a high velocity projectile, a phenomenon known as hydraulic ram effect, created by the passage of the projectile through the fluid often causes massive damage to the tank. This study was conducted to continue experimental investigation of the attenuation of the hydraulic ram effect through addition of a gas to a fuel-foam mixture.

The tests were conducted using two types of projectile (½ in. steel spheres and 0.50 caliber ogival projectiles) which were fired into a test tank. The tank was filled first with water and then a water/Pneumacel mixture. Four pressure transducers were located in the back wall of the tank and two pressure transducers were located inside the tank to measure the pressure pulses.

The initial pressure pulse caused by the projectile moving through the water alone was measured during the first series of tests. A significant reduction in this pressure was noted during the second series in which the water/Pneumacel mixture was used. It was also found that a projectile moving through the fluid creates a cavity in its wake. When the cavity collapses, a pressure wave is generated. The cavity created by the passage of the spheres through the fluid was small and the pressure wave generated by its collapse was insignificant when compared to the initial pressure wave. However, the pressure wave created by the collapse of the cavity behind the ogival projectile was approximately the same magnitude as the initial pressure wave. It appears that this second pressure wave may be a major contributor to massive fuel tank damage. During the second series of tests (water/Pneumacel mixture), this pressure wave was significantly reduced.

DD FORM 1 NOV 65 1473

1a

UNCLASSIFIED
Security Classification

KEY WORDS	LINK A		LINK B		LINK C	
	ROLE	WT	ROLE	WT	ROLE	WT
Hydraulic Ram Effect						
Aircraft Fuel Tanks						

GA/MC/73-3

AN EXPERIMENTAL STUDY OF ATTENUATION OF SHOCK WAVES IN AIRCRAFT FUEL TANKS

THESIS

GA/MC/73-3 John R. Breuninger, Jr.
Captain USAF

Approved for public release; distribution unlimited.

ic

GAP/AA/73-3

AN EXPERIMENTAL STUDY OF ATTENUATION OF SHOCK WAVES IN AIRCRAFT FUEL TANKS

THESIS

Presented to the Faculty of the School of Engineering
of the Air Force Institute of Technology
Air University

In Partial Fulfillment of the
Requirements for the Degree of
Master of Science

by

John R. Breuninger Jr., BS
Captain USAF

Graduate Astronautical Engineering
June 1973

Preface

This report represents a continuation of experimental studies of the hydraulic ram effect and its effect on aircraft fuel cell survivability. I hope that the information contained in this report will lead to further research and development in the area of fuel cell survivability.

I wish to thank many individuals without whose support this research would not have been possible.

Specifically, I want to thank Dr. Peter J. Torvik, my thesis advisor; Major James Wade of the Survivability Division of the Air Force Flight Dynamics Laboratory; Mr. L. Gilbert and the Survivability Test Group of the Air Force Flight Dynamics Laboratory; and Dr. Bernard Lavery of the Du Pont Corporation who supplied the Pneumacel and furnished information concerning it.

I also wish to thank Mr. Charles Anderson, Mr. Raymond Settles, and SSgt. Karl Aune for the many hours they spent helping me find and fabricate equipment and conduct the tests.

And most of all I wish to thank my wife, Mary Elizabeth, who spent many hours reading rough drafts and running our home while I was doing this work.

John R. Breuninger Jr.

GA/MC/75-3

Preface

This report represents a continuation of experimental studies of the hydraulic ram effect and its effect on aircraft fuel cell survivability. I hope that the information contained in this report will lead to further research and development in the area of fuel cell survivability.

I wish to thank many individuals without whose support this research would not have been possible.

Specifically, I want to thank Dr. Peter J. Torvik, my thesis advisor; Major James Wade of the Survivability Division of the Air Force Flight Dynamics Laboratory; Mr. L. Gilbert and the Survivability Test Group of the Air Force Flight Dynamics Laboratory; and Dr. Bernard Lavery of the Du Pont Corporation who supplied the Pneumacel and furnished information concerning it.

I also wish to thank Mr. Charles Anderson, Mr. Raymond Settles, and SSgt. Karl Aune for the many hours they spent helping me find and fabricate equipment and conduct the tests.

And most of all I wish to thank my wife, Mary Elizabeth, who [illegible] many hours reading rough drafts and running our home while I was doing this work.

John R. Breuninger Jr.

Contents

List of Tables

List of Figures

List of Figures

Abstract

When a full, or partially full, aircraft fuel tank is penetrated by a high velocity projectile, a phenomenon known as hydraulic ram effect, created by the passage of the projectile through the fluid, often causes massive damage to the tank. This study was conducted to continue experimental investigation of the attenuation of the hydraulic ram effect through addition of a gas to a fuel-foam mixture.

The tests were conducted using two types of projectile ($\frac{1}{2}$ in. steel spheres and 0.50 caliber ogival projectiles) which were fired into a test tank. The tank was filled first with water and then a water/Pneumacel mixture. Four pressure transducers were located in the back wall of the tank and two pressure transducers were located inside the tank to measure the pressure pulses.

The initial pressure pulse caused by the projectile moving through the water alone was measured during the first series of tests. A significant reduction in this pressure was noted during the second series in which the water/Pneumacel mixture was used. It was also found that a projectile moving through the fluid creates a cavity in its wake. When the cavity collapses, a pressure wave is generated. The cavity created by the passage of the spheres through the fluid was small and the pressure wave generated by its collapse was insignificant when compared to the initial pressure wave. However, the pressure wave created by the collapse of the cavity behind the ogival projectile was approximately the same magnitude as the initial pressure wave. It appears that this second pressure wave may be a major contributor to massive fuel tank damage. During the second series of tests (water/Pneumacel mixture), this pressure wave was significantly reduced.

GA/MC/73-3

AN EXPERIMENTAL STUDY OF ATTENUATION OF SHOCK WAVES IN AIRCRAFT FUEL TANKS

I. Introduction

Background

In recent years, a great deal of work has been accomplished in the area of aircraft fuel tank (or fuel cell) survivability. Reticulated polyurethane foam has been developed and placed in fuel cells to reduce the possibility of fire or explosion if the empty, or partially empty, fuel cell is struck with an incendiary bullet. Self-sealing bladders have also been developed to seal a small fuel cell rupture.

However, during development and testing of these fuel cell survivability devices it was discovered that a full, or nearly full, fuel cell was susceptible to massive damage when struck by a high velocity projectile. Even small calibor (i.e., 0.50 caliber) projectiles caused such extensive damage that the self-sealing fuel cell bladders were unable to seal the rupture.

Such a massive failure can lead to several modes of aircraft kill. Fuel starvation if a main tank is ruptured, fire or secondary explosion within the aircraft, or damage to critical aircraft systems are all possible if a severe fuel cell rupture is present.

Hydraulic Ram Effect. The phenomenon which causes this massive rupture of the fuel cell is the hydraulic ram effect. The hydraulic ram effect is actually a series of events which are related and, in actual occurrence, overlap each other. Seaberg and Bristow (Ref 6), the Northrop Corporation (Ref 5), and Bristow (Ref 2) agree that there

are 5 basic events: (1, the shock wave generated by the projectile initially penetrating the front wall of the fuel cell, (2) the continuous generation of a pressure field as the projectile passes through the fluid, (3) the pressure rise caused by the tumbling of the projectile, (4) the build-up of pressure on the back wall as the projectile approaches the wall, (5) the creation and collapse of a large cavity behind the projectile.

Some analytic studies of the hydraulic ram effect have been performed. Seaberg and Bristow (Ref 6) analyzed the effect using simple drag theory and energy transfer theory. While this approach was adequate to model the passage of the projectile through the fluid, it was too simple to completely describe the other interrelated effects of the hydraulic ram. Albersen (Ref 1) used a blast wave theory to approximate the peak pressure within the fluid and a rigid-plastic plate theory to analyze the exit wall region of the tank. However, if each event is analyzed individually, a possible synergistic effect due to the complex interplay of the various hydraulic ram effects is lost.

Other studies that have been performed have used an experimental trial-and-error approach. In most cases, understanding the hydraulic ram effect from a macroscopic view and determining what could be done to reduce the effect were the goals of the experiments. Stepka (Ref 7) conducted some experiments with high velocity projectile impacts of a water filled tank. This study was performed during 1965 and was conducted to understand and measure the basic hydraulic ram effect. Northrop (Ref 5) also conducted hydraulic ram studies, but these were accomplished to provide specific information for construction of a fuel cell which would withstand the ram under certain conditions.

In 1970, Winters (Ref 11) conducted a study of the hydraulic ram effect as a thesis project for the Air Force Institute of Technology. Then in 1972, Clark (Ref 3) attempted to obtain some baseline data on the hydraulic ram effect. He conducted experimental tests in which a hydraulic ram was generated by firing ½ inch spherical balls at high (2700 ft per second) velocity into a 2 foot water-filled tank. The pressure field generated by the passage of the spheres through the water was measured. Then, having obtained a known data base, Clark attempted to attenuate the shock waves by using a known quantity of gas dispersed throughout the water. The results were encouraging and further testing was recommended.

Purpose and Scope. The purpose of this study was to further investigate the attenuation of the hydraulic ram effect by use of a known quantity of gas dispersed throughout the fuel cell. Clark (Ref 3) used only ½ inch spherical balls as projectiles to eliminate any variation in data due to the possible tumbling of an ogival projectile. All pressure readings were from off centerline locations because a spherical shock was assumed.

As a projectile moves through a fluid, it continually generates a pressure field. It has been conjectured that as the projectile approaches the back wall, this field might build up, causing a high pressure just prior to impact. For this reason, pressure readings in the present study were taken at the back wall as close as possible to the impact point. Also, a pressure wave, generated by the collapse of the cavity created by the passage of the projectile through the fluid, impacts the front and rear walls which have been weakened by the passage of the projectile through the tank. It is expected that this pressure wave may be a major contributor to tank wall failure. Therefore, gages were also placed in the tank interior as close to centerline as possible in order to measure the pressure generated by the cavity collapse.

The experiment was divided into two series. The first series used projectiles impacting a tank filled with water to establish a data base and to compare data with previous results. The second used a water/foam mixture to attenuate the hydraulic ram effect. Each test series used both spherical and ogival projectiles.

An additional experiment was carried out during the first series of tests. Four blow-out plugs were placed in the rear wall and attempts were made to determine the velocity with which these plugs were ejected. It was reasoned that the pressure wave would impinge on the plugs and the impulsive force could be measured through a force/momentum exchange. Calculations for this exchange can be found in Appendix B.

II. Experimental Apparatus

Target Materials

Water was the target material used during the first series of tests. Testing with water yielded results which formed a baseline both for comparison with test data from previous experiments and for evaluation of the shock attenuation of the mixture.

The target material used in the second series of tests was a water/Pneumacel mixture. Pneumacel is a multi-fiber, Dacron material commercially produced by the Du Pont Company as carpet padding. Pneumacel was selected by Clark (Ref 3, 8) during his experiments in shock attenuation because it is an open fiber material which contains a controlled amount of gas. Pneumacel is not particularly recommended for use in fuel cells. For one reason, petroleum products will dissolve the bonding agent used to hold the Pneumacel together. For another, Pneumacel reduced the available volume of the test tank by 18%, compared with a tank reduction of 7% for reticulated polyurethane fire-retardent foam. Information concerning the physical properties of Pneumacel can be found in Appendix A.

Apparatus

The experiment was conducted in the Air Force Flight Dynamics Laboratory (AFFDL), Gun Range Number 1. In order to establish a baseline against which previous experimental data could be compared, the initial shots in each of the two series (water alone as a target material and water/Pneumacel as a target material) were conducted using $\frac{1}{2}$ in. steel balls as projectiles. The final shots in each series were conducted using standard 0.50 caliber ogival projectiles. Figure 1 shows the general layout of the principal components of the test apparatus: (1) the gun mount, (2) the projectile velocity measuring system, (3) the oscilloscope triggering system, (4) the target, (5) the plug velocity measuring system.

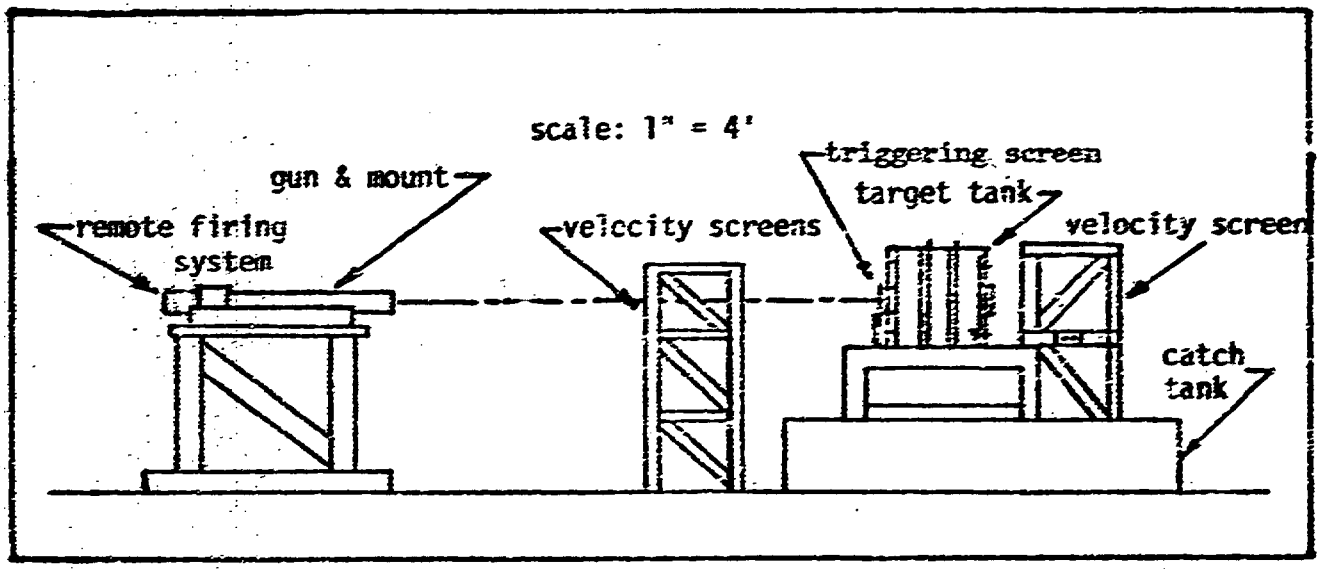

Figure 1

General Apparatus Layout

The gun used in the initial shots of each series was a smooth-bore, 0.50-caliber, test barrel attached to a Frankford mount. The test barrel was 95½ in. long and the actual bore was 0.502 in. in diameter. The projectiles were standard ½ in. stainless steel ball bearings. All bearings were 0.497 in. in diameter and weighed 129.1 grains.

The gun used in the final shots of each series was a rifled-bore, 0.50-caliber, test barrel mounted on a Frankford mount. The test barrel was 34 in. long and the actual bore was 0.502 in. in diameter. The projectiles were standard 0.50 caliber ball rounds. A 0.50 caliber ball round is actually an ogival projectile constructed of soft steel with a brass jacket. Each projectile weighed 699.8 grains.

The same breech and bolt were used with both barrels. The breech was screwed into the aft end of the barrel and the bolt was attached to the aft end of the breech. The bolt had a solenoid-activated firing pin which could only be triggered from the control room. The cartridge was attached to the bolt and the assembly was then attached to the breech. In order to prevent accidental discharge of the gun while personnel remained in the tunnel, three switches had to be activated before the gun would fire. The first switch was on the bolt and was turned from the safe to the armed position after the bolt had been placed in the breech. The second switch was located outside the tunnel entrance and was activated by the last man leaving the tunnel. This switch also activated warning lights by the tunnel entrance and in the control room. The third switch was located in the control room and, when activated, closed the circuit and fired the gun.

Between the muzzle of the gun and the target were two velocity screens, exactly 2 feet apart. The screens were constructed of paper

crisscrossed with a continuous horizontal strip of metallic paint. The strip was $\frac{1}{32}$ in. wide and the separation between each strip was $\frac{1}{4}$ in. The paper was mounted between 2 plates and a 90 volt D.C. charge was applied across the plates through the strip on the paper. When the projectile passed through the paper, the circuit was broken and a triggering pulse was generated. The screens were connected to Beckman timers and the elapsed time between successive projectile impacts was measured.

A single screen was mounted 2 in. in front of the target. The pulse generated by the projectile passing through this screen was used to trigger the sweep of the oscilloscopes.

The target was a rectangular tank 24 in. high, 30 in. wide, and 24 in. deep. The top, bottom, and sides were $\frac{1}{4}$ in. steel plates, reinforced with 2 bands of $2\frac{1}{2} \times 1\frac{3}{4}$ steel angle iron. The front plate was removable and was made of $\frac{1}{8}$ in. 2024 aluminum. The plate was held to the tank with eighteen $1\frac{1}{2}$ in. "C" clamps. Zinc chromate was used as a sealant between the plate and the tank. A 4 in. diameter hole was cut in the center of the plate and a $1\frac{1}{4}$ in. wide circular collar was used to hold an 8 mil sheet of plastic over the opening. Eight sheet metal screws attached the collar to the plate and a bead of zinc chromate was also used to seal the collar to the plate.

The back plate was also removable and was made of $\frac{1}{2}$ in. 2024 aluminum. This plate was held to the tank by twenty-one $1\frac{1}{2}$ in. "C" clamps. Zinc chromate was also used as a seal between the plate and the tank. A 6 in. square hole was cut in the center of the back plate and an 8 in. square plate of $\frac{3}{4}$ in. 2024 aluminum was mounted to the back plate. Sixteen $\frac{1}{4}$ in. bolts were used to attach the square to the

back plate. General Electric RTV® sealant was used to seal the sauare to the back plate. Figure 2 shows the transucer and blow-out plug arrangement on the 8 in. square plate.

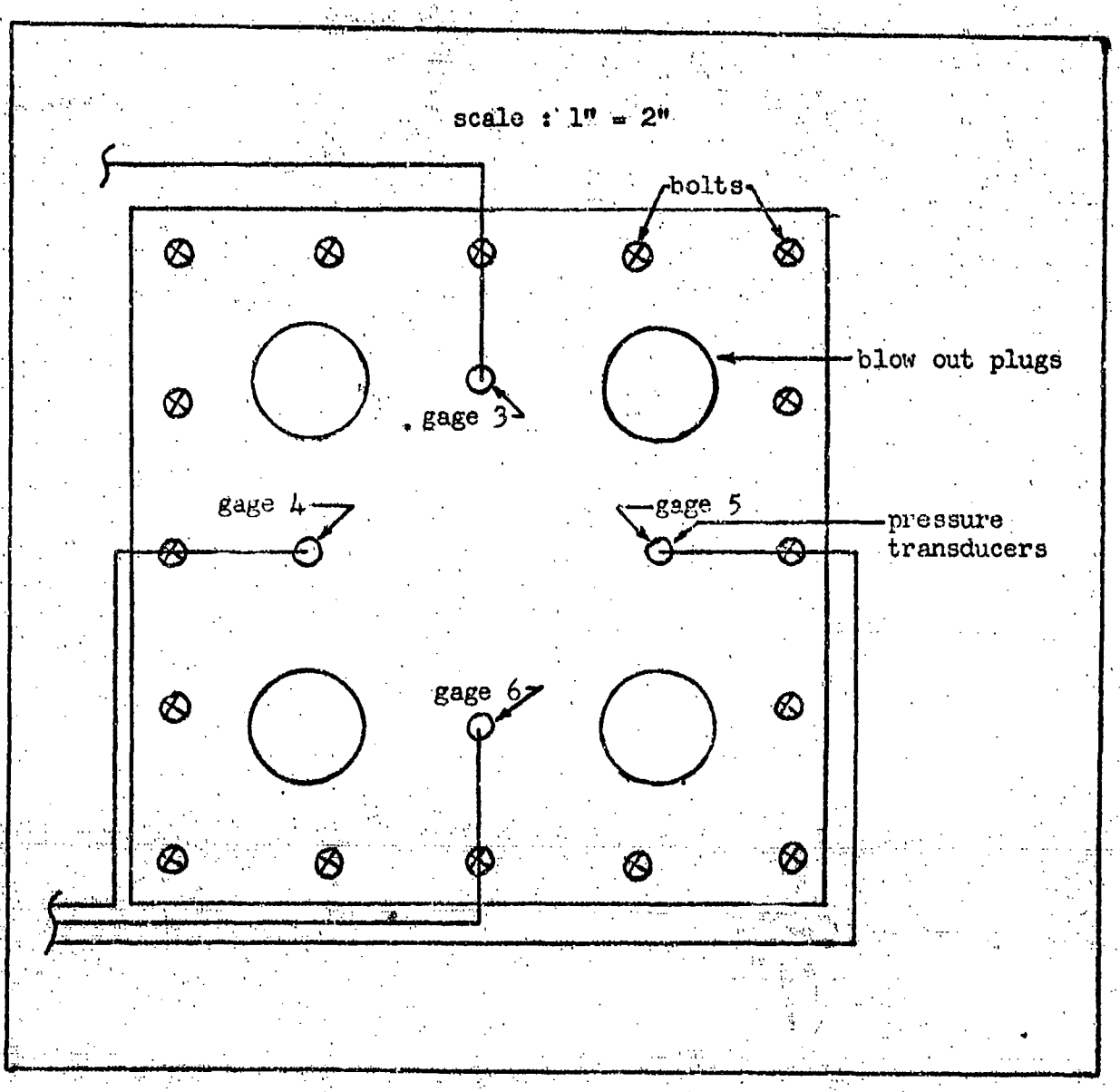

Figure 2

Transducer and Blow Out Plug Arrangement

Four conical blow-out plugs were placed in the square plate, 45° to either side of the vertical centerline, and 2.82 in. from the center of the 8 in. square plate. The plugs were constructed of 2024 aluminum and were truncated cones. The conical taper of each plug was 30°, the top surface was $\frac{1}{2}$ in. in diameter. Each was $\frac{3}{4}$ in. long and weighed 405 grains. They were sealed and held in place against the static water pressure by G-395 type aircraft grease. Figure 3 shows a side view of the plugs.

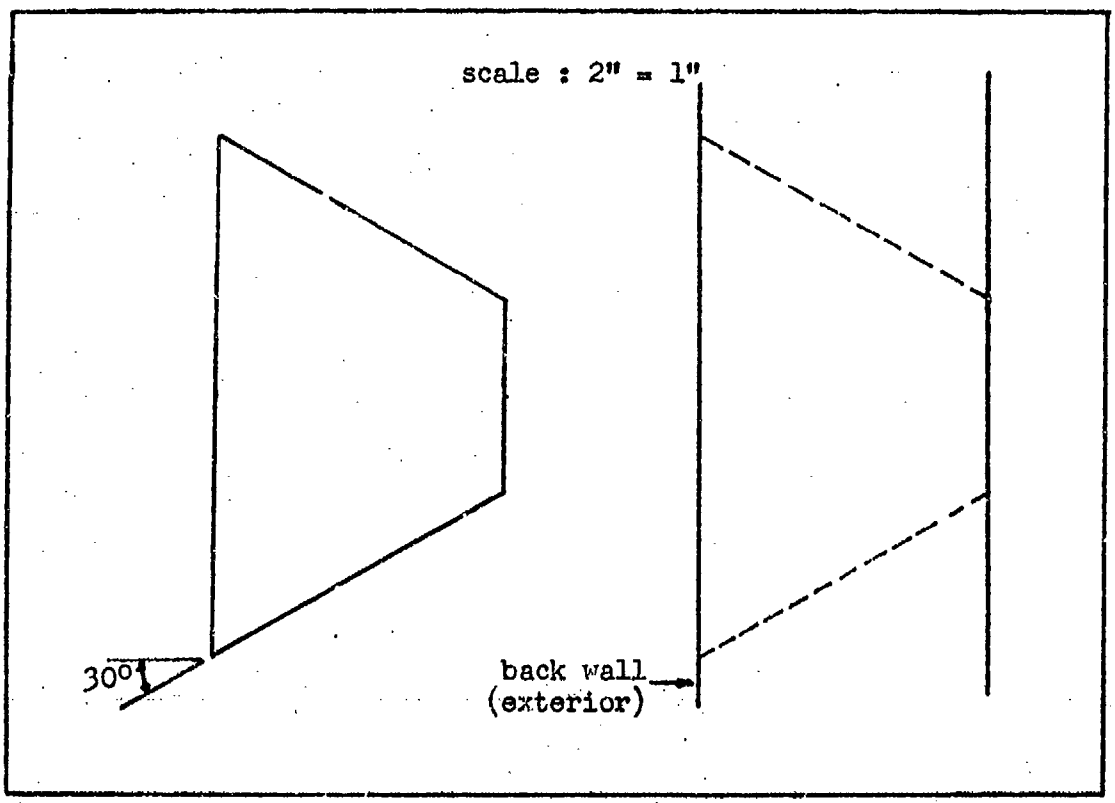

Figure 3

Blow Out Plug (Side View)

Four Kistler 202A1 pressure transducers were mounted on the vertical and horizontal centerlines, 2 in. from the center of the plate. They were threaded into the plate and the pressure sensing faces of the transducers were flush with the inside wall of the square plate. This arrangement was chosen so that at least 2 gages would be close to the projectile impact point.

Two other Kistler 202A1 pressure transducers were mounted inside the tank by $\frac{1}{2}$ in. aluminum tubing and fittings. Both gages were mounted so that the pressure sensing face of the gage was pointed 180° to the path of the projectile and on the horizontal centerline. These gages were on opposite sides of the vertical centerline, 6 in. from the projectile path and 12 in. forward of the 8 in. square plate, i.e., at 12 in. from the surface of entry. These gages were used to record the collapse of the cavity generated by the passing projectile.

Two velocity screens were mounted behind the tank. These screens were exactly 2 feet apart and the forward screen was $5\frac{7}{8}$ in. from the back face of the 8 in. square plate. These screens were used to measure the velocity of the blow-out plugs.

A wooden catch tank, $8\frac{1}{2}$ ft. long, $3\frac{1}{2}$ ft. wide, and $1\frac{1}{2}$ ft. deep, lined with a plastic sheet, was used to catch the water spilled when the target tank was ruptured by the projectile.

Instrumentation

Kistler 202A1 pressure transducers connected with microdot coaxial cables to Kistler Model 504D dual mode amplifiers were used

to measure the pressure. The back plate was drilled and tapped and the transducers were threaded into the plate. The two transducers inside the tank were mounted in an adapter used by AF Flight Dynamics Laboratory for Kistler gages.

All pressure data was displayed on three Tektronix 5103 N/D12 dual beam oscilloscopes. Two pressure readings were displayed on each scope. The scopes were triggered by a screen mounted 2 in. in front of the tank and a single sweep was used. The data was recorded using Polaroid type 47 high-speed film.

The signals generated by the passing projectiles on the front and rear velocity screens were recorded on two Beckman model 7360A universal timers. The passage of a projectile through the first velocity screen started the timer and the passage through the second screen stopped the timer. The readings were in microseconds and were then converted to feet per second.

III. Experimental Procedures

Forty four shots were fired during the experiment. The first 18 shots were fired to establish a cartridge loading procedure and to establish a powder charge versus projectile velocity curve. The $\frac{1}{2}$ in. steel balls were loaded in a modified 0.50 caliber cartridge in the following manner:

1) the primer charge was attached to the cartridge.

2) the powder for the desired projectile velocity was weighed and poured into the cartridge.

3) two strips of teflon tape, $\frac{1}{2}$ in. wide and 2 in. long, were placed over the end of the cartridge, the second strip perpendicular to the first.

4) the $\frac{1}{2}$ in. steel ball was placed on the tape and then rammed into place snugly against the powder charge.

Using this technique, the teflon tape kept the ball snugly in place and also acted as wadding to prevent gas flow-by as the ball moved out of the cartridge and down the gun barrel.

The first series of 16 test shots was conducted using water as the target material. The projectile used for the first 13 shots was the $\frac{1}{2}$ in. steel ball. The initial velocity was 1000 feet per second. Succeeding velocities were incrementally increased to a maximum of 3091 feet per second. During these shots, the recording equipment was tuned and the refurbishing procedures between shots were established.

The last 3 shots of the first series were conducted using standard 0.50 caliber projectiles. The muzzle velocity was 2720 ± 50 feet per second.

The second series consisted of 10 shots which were fired into a water/Pneumacel mixture. The projectile used in the first 5 shots was the $\frac{1}{2}$ in. steel ball. All shots were conducted using a full powder charge which resulted in a projectile velocity of 2790±40 feet per second. The next 5 shots were conducted using the standard 0.50 caliber projectile. Again a full powder charge was used which resulted in a projectile velocity of 2613±75 feet per second.

The procedure for each shot was as follows:

1) the cartridge was loaded for the velocity required.

2) the instrumentation was turned on to warm up.

3) the four blow-out plugs were put in place as required.

4) the plastic sheet covering the impact point was replaced.

5) the tank was filled with water.

6) the front, rear, and triggering velocity screens were put in place and the circuit to each turned on.

7) one at a time the circuit to each of the five velocity screens (2 in front, 2 in the rear, 1 triggering) was broken to insure that the screens were functioning properly.

8) the three oscilloscopes were set on single sweep delay.

9) the Polaroid cameras were attached to each oscilloscope.

10) the Beckman timers were reset to zero.

11) the cartridge was placed in the remote firing bolt, which was then secured to the breech of the test gun.

12) the switch on the bolt was switched from safe to arm.

13) the tunnel was evacuated and the safety switch was activated.

14) the shutters of the three cameras were opened.

15) the firing switch was activated.

16) following the shot, the safety switch was turned off, the remote firing bolt was switched from arm to safe, and the bolt was removed from the gun breech.

17) the Polaroid pictures were marked as to shot number and scope, and the velocity data from the front and rear screens was noted.

18) during the shots with the Pneumacel, the projectile passage through the Pneumacel left a 1 $\frac{1}{2}$ in. hole which was repacked with Pneumacel to the same density as the original material. Two inch squares of Pneumacel were cut, placed in the hole, and pushed into place.

IV. Results and Discussion

Results

Sixteen test shots were conducted during series 1 (water only). No data from shots numbered 2, [illegible], and 9 were obtained because of faulty triggering of the oscilloscopes. The data for the 13 successful shots were displayed on three dual beam oscilloscopes and were recorded on Polaroid photographs as shown in Figure 4. The traces run from left to right. Positive pressure is read below the zero reference line. The time reference is from the passage of the projectile through the velocity screen located 2 in. in front of the tank entry point. At a muzzle velocity of 2700 ft/sec, the time between passage of the projectile through the velocity screen and target impact is 0.061 milliseconds. One large division on the Polaroid photograph is equal to 1 cm. The Polaroid photographs for the 13 successful shots in series 1 are shown in Figures 15-27 in Appendix C.

Tabulation of the projectile velocity, back wall impact time, peak pressure at the back wall, and peak pressure generated by the cavity collapse for series 1 is shown in Table I. The back wall impact time was obtained from the Polaroid scope pictures. The traces show an increasing positive pressure followed by a series of positive and negative pressure spikes around the zero pressure reference line. It was assumed that the return of the trace to the zero reference line and the positive/negative spikes were caused by the projectile impacting the back wall causing the gages in the wall to "ring." The impact

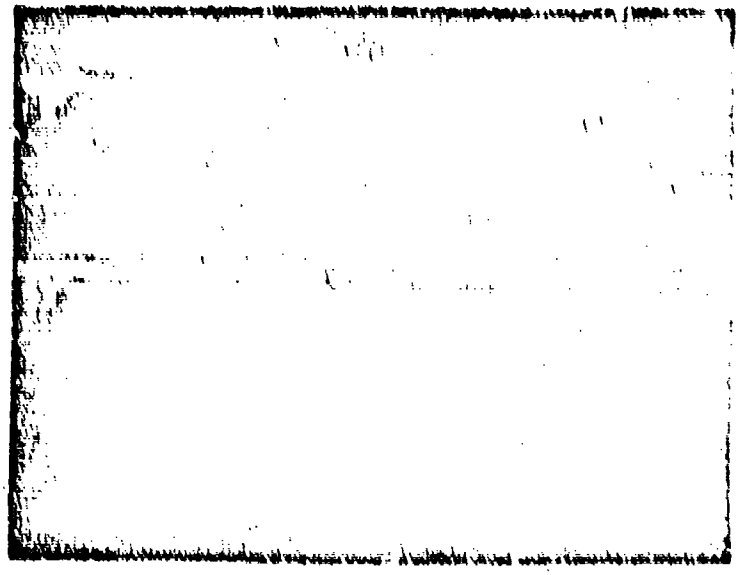

Shot 8.

Water

Gages 1 & 2, 5 msec/cm
100 psi/cm

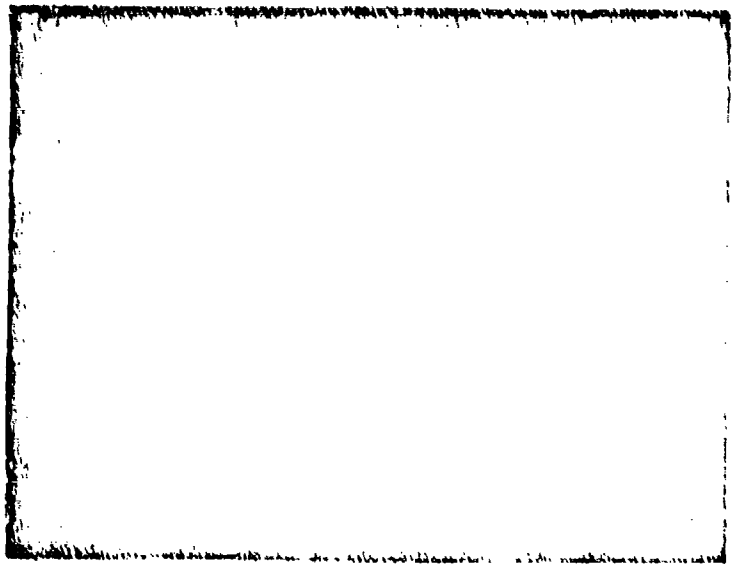

Gages 3 & 4, 0.5 msec/cm
100 psi/cm

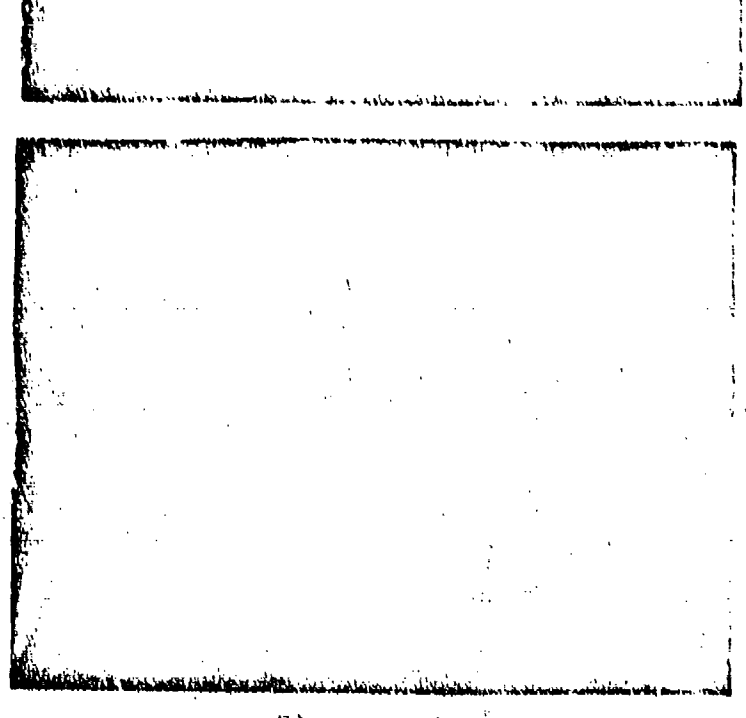

Gages 5 & 6, 0.5 msec/cm
100 psi/cm

Projectile velocity-
2296 fps

Figure 4
Scope picture, Series 1, Part 1, Shot 8

Table I

Tabulated Results of Series 1

Shot	Impact Velocity (fps)	Back Wall Impact (mses)	Inside Tank		Back Wall			
			Gage 1 (psi)	Gage 2 (psi)	Gage 3 (psi)	Gage 4 (psi)	Gage 5 (psi)	Gage 6 (psi)
1*	1000	5.8	40	40	30	40	ND	ND
2*	NO DATA							
3*	1700	2.8	ND	ND	ND	ND	40	ND
4*	NO DATA							
5*	1391	3.6	20	20	ND	50	ND	ND
6*	1406	3.6	ND	20	ND	50	ND	ND
7*	2037	2.5	20	20	ND	100	ND	ND
8*	2396	2.2	20	20	ND	130	ND	ND
9*	NO DATA							
10*	2739	1.9	20	20	ND	190	ND	ND
11*	2928	1.7	ND	ND	ND	170	ND	140
12*	2928	1.7	ND	ND	ND	120	ND	140
13*	3091	1.7	30	20	ND	150	ND	130
14**	2770	0.7	520	520	630	630	ND	630
15**	2691	0.7	ND	ND	ND	570	590	590
16**	2680	0.8	ND	ND	ND	800	800	ND

* 1/2 in. spherical projectile

** 0.50 caliber ogival projectile

ND No data on that gage

time was taken as the interval from the start of the trace to the point where the trace began to return to the zero reference line. The impact times for the spherical projectiles decrease as velocity increases. However, the impact time for the ogival projectiles is approximately $\frac{1}{2}$ the time for the spherical projectiles fired at the same velocity. The ogival projectiles have the same cross-sectional diameter as the spherical projectiles, but they have 5.5 times the mass (and thus 5.5 times the kinetic energy at the same velocity). If the ogival projectile did not tumble, the larger kinetic energy and momentum of the ogival projectile coupled with an equivalent drag for both projectiles would result in less deceleration for the ogival projectile and a consequent lower back wall impact time. However, as is shown later, the ogival projectile does tumble, presenting a larger area to the fluid. Because this increase in area results in an increase in drag, the impact time should be higher than it is, unless the tumbling does not occur until the projectile is almost through the tank. As is indicated in the subsequent Discussion section, this is the case. Peak pressure in the fluid at the back wall was taken from the Polaroid pictures of gages 3, 4, 5, and 6. The time scale is very small (0.5 msec/cm) so that the pressure build up on the back wall could be seen. The peak pressure generated by the cavity collapse was taken from the Polaroid pictures of gages 1 and 2. The time scale for these gages was larger than that for gages 3-6 in order to insure the recording of the cavity collapse. However, the

time scale was still only 5 msec/cm. The pressure at gages 1 and 4 due to the passing projectile (not tabulated) were in good agreement with the peak pressure at the back wall.

Ten test shots were conducted during series 2 (water/Pneumacel). The Polaroid photographs for the 10 shots are shown in Figures 28-37 in Appendix C. Tabulation of the projectile impact velocity, back wall impact time, peak pressure in the fluid at the back wall, and peak pressure generated by the cavity collapse for series 2 is shown in Table II.

Discussion

Series 1. The first 13 shots of series 1 were conducted using ½ in. steel spheres as projectiles. Projectile velocity was progressively increased from 1000 ft/sec to 3091 ft/sec. A graph of the peak pressure at the wall versus projectile velocity is shown in Figure 5. The 10 shots on which data were successfully collected show an increase in peak pressure at the back wall as velocity increases, a reduction in the back wall impact time, and an almost constant cavity collapse pressure. As can be seen from Figure 5, a fair correlation exists between the peak pressure at the back wall and the experimental data obtained by Clark (Ref 3). The difference in data might be due to the fact that the gages in this study were mounted in the back wall (i.e., 2 ft. from the impact point) and were only 2 in. from centerline. The gage used by Clark from which the data in Figure 5

Table II

Tabulated Results of Series 2

Shot	Impact Velocity (fps)	Back Wall Impact (msec)	Inside Tank		Back Wall			
			Gage 1 (psi)	Gage 2 (psi)	Gage 3 (psi)	Gage 4 (psi)	Gage 5 (psi)	Gage 6 (psi)
1A*	2750	1.6	0.0	0.0	0.0	0.0	0.0	0.0
2A*	2750	1.5	0.0	0.0	0.0	0.0	0.0	0.0
3A*	2750	1.6	0.0	0.0	0.0	0.0	0.0	0.0
4A*	2750	1.5	0.0	0.0	ND	0.0	0.0	0.0
5A*	2830	1.4	0.0	0.0	ND	0.0	0.0	0.0
6A**	2680	1.0	0.0	0.0	ND	0.0	0.0	0.0
7A**	2660	0.9	0.0	0.0	ND	ND	0.0	0.0
8A**	2645	1.0	20	10	ND	ND	0.0	0.0
9A**	2538	1.2	30	30	ND	ND	0.0	0.0
10A**	2688	0.9	20	10	ND	ND	0.0	0.0

* 1/2 in. spherical projectile

** 0.50 caliber projectile

ND No data on that gage

was obtained was 8.7 in. from centerline but was only 9 in. from the impact point. If the spherical projectile had moved with a constant velocity through the tank, at an impact velocity of 1000 ft/sec, back wall impact should have occurred at 2.0 msec. In fact, back wall impact occurred at 5.8 msec for an impact velocity of 1000 ft/sec. Thus, the spherical projectile slowed appreciatively during its passage through the tank, and a pressure gage located near the impact point should read a higher pressure than one farther away. This is also verified by Clark's data. The pressure reading from the gages located even closer to the impact point are higher than the gage used for comparative purposes. This gage was selected because it was the closest to the back wall. However, as can be seen on Figure 5, the pressure generated by the cavity collapse is independent of velocity. It might be assumed that since the pressure at the back wall increases with velocity and the pressure generated by the collapse of the cavity remains constant at a much lower value, the damage causing mechanism is the initial pressure wave. In the case of spherical projectiles this is the case. The separation of the flow caused by the passage of the sphere through the fluid is minimal and the cavity which is created by this separation is small. Thus, the collapse of this cavity creates a weak pressure field.

The second set of shots in series 1, a total of three, was conducted using 0.50 caliber ogival projectiles. The projectiles had about 5.5 times the mass of the steel balls. For the same impact

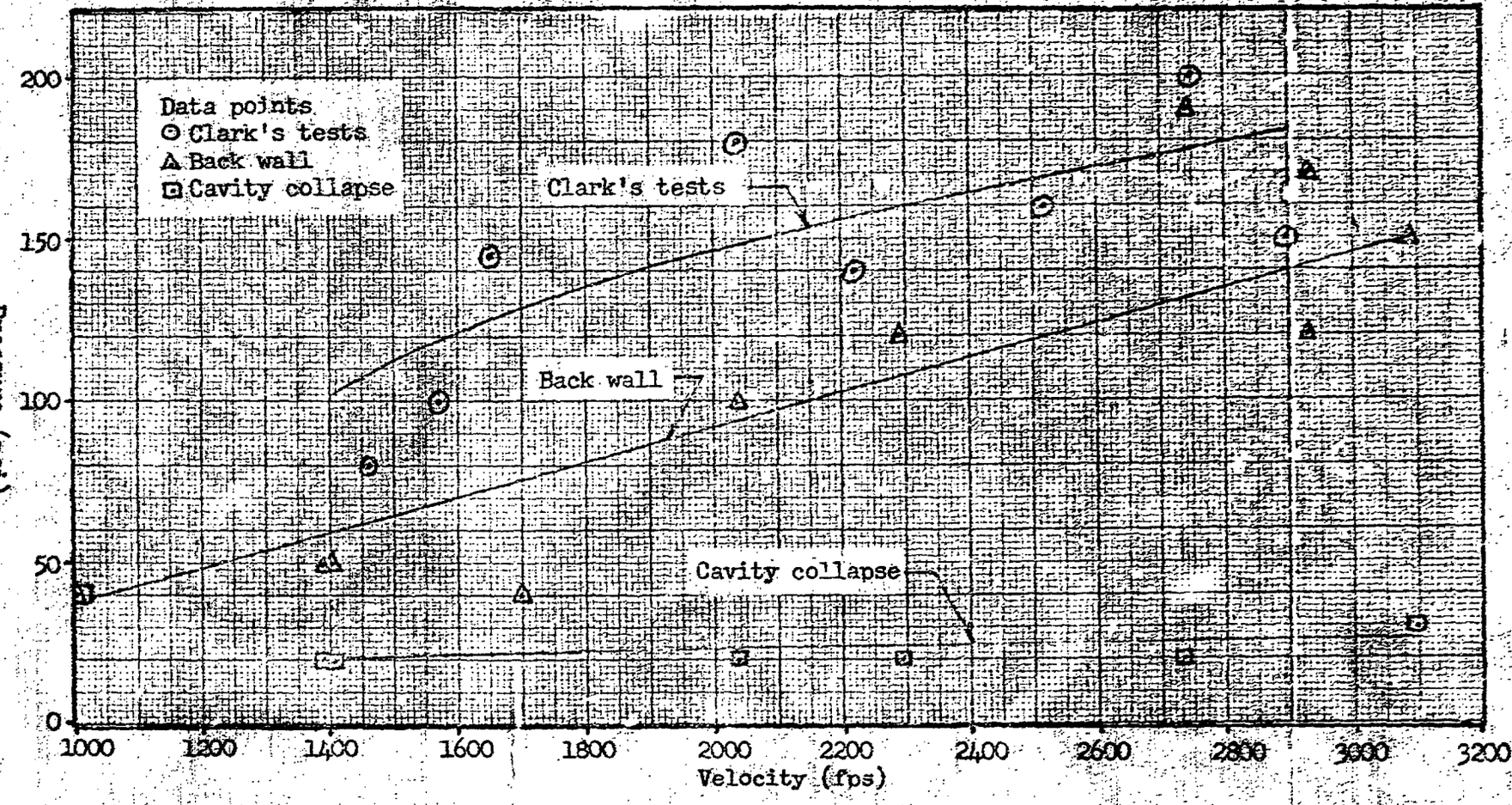

Figure 5, Impact Velocity vs Pressure
(Series 1, Spherical Projectiles Only)

velocity, the peak pressure at the wall was about four times the peak pressure generated by the steel balls moving through the fluid. However, the pressure generated by the collapse of the cavity was approximately 500 psi, or 25 times the cavity collapse pressure generated by the steel balls.

A large cavity was created because as the projectile moved through the fluid it tumbled, presenting a larger surface area to the fluid. The tumbling of the projectile can be seen in Figures 6-9. These stills were obtained from a high speed film taken by the Air Force Flight Dynamics Laboratory (AFFDL) on 3 June 1970. The film was taken during a test conducted by AFFDL in which 0.50 caliber ogival projectiles were shot into a 2 ft test cube filled with water. The projectile impact velocity was 2686 ft/sec and it impacted the tank perpendicular to the front face. In Figure 6, the projectile is 1 ft. into the tank. Figure 7 shows the projectile approximately 14 in. into the tank and just beginning to tumble.

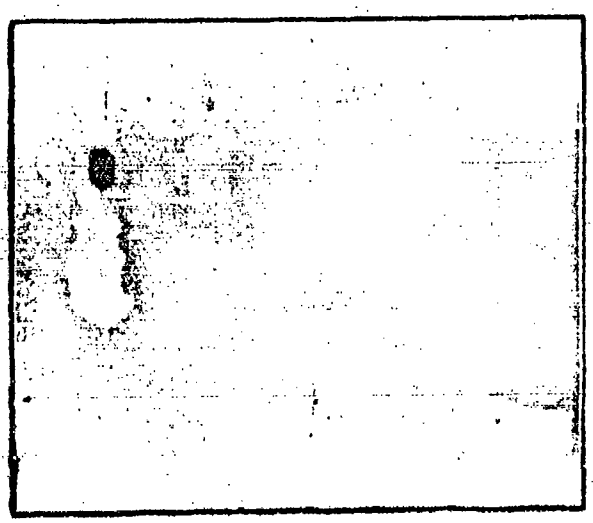

Figure 6, Ogival Projectile in Test Tank

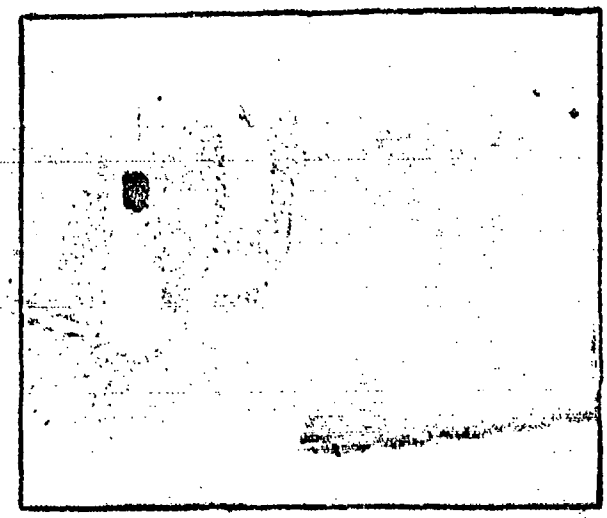

Figure 7, Ogival Projectile in Test Tank

As can be seen in Figure 8, the projectile is 15 in. into the tank and has now tumbled 90°. Note the large cavity behind the projectile. Figure 9 shows that the projectile is now 17 in. into the tank but that it is still rotated 90°. The cavity has grown larger still.

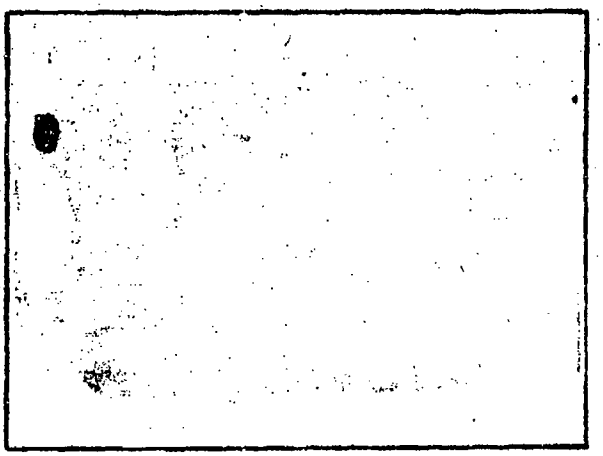

Figure 8, Ogival Projectile in Test Tank

Figure 9, Ogival Projectile in Test Tank

During every shot conducted in this test, a large cavity was created when the projectile tumbled. On only one of the nine shots conducted, the projectile failed to tumble. In that case, the cavity which was created was very small (Ref 9).

Thus it was assumed that the projectile tumbled during the second set of shots in series 1, and that this tumbling created the large cavity, the collapse of which was recorded on gages 1 and 2.

Visual observations of the target during impact by the 0.50 caliber ogival projectiles showed that the plastic covering the 3 in. impact hole was blown out and water was blown out of the hole with sufficient force to spray it 12-15 feet up the tunnel. No such effect was noted during the tests using $\frac{1}{2}$ in. spheres as projectiles.

Series 2. The first set of 5 shots in series 2 (water/Pneumacel) were conducted using $\frac{1}{2}$ in. steel spheres as projectiles. Because the higher peak pressures were recorded during part 1 of series 1 only at the higher velocities, all 5 shots were conducted at nominal muzzle velocities of 2700 ft/sec. Higher pressures were desired during series 2 so that any possible attenuation effects of Pneumacel might be observed.

A comparison of the peak pressures during this test and the peak pressures obtained by Clark (Ref 3) is shown in Figure 10. There was no measurable pressure field generated by the collapse of the cavity. Because the only difference between the first sets of series 1 and series 2 was the inclusion of Pneumacel in the test tank, either the Pneumacel prevented the formation of the cavity or completely attenuated the pressure field generated by the cavity.

The next set of 5 shots in series 2 was conducted using 0.50 caliber ogival projectiles fired at full muzzle velocity (2650 ft/sec nominally). There was no pressure measured at the back wall prior to the time the projectile impacted the back wall. And while there was a pressure field generated by the cavity collapse, it was only 20-30 psi, compared with 500 psi without the Pneumacel present.

During set 2 of series 1, the cavity collapse pressure blew out the plastic covering of the impact hole. In the experiments with a Pneumacel filled tank, the plastic remained intact except for the hole made by the projectile entering the tank and there was no water blown up the tunnel. These observations are taken as further confirmation of the fact that the Pneumacel significantly reduced the hydraulic ram effect.

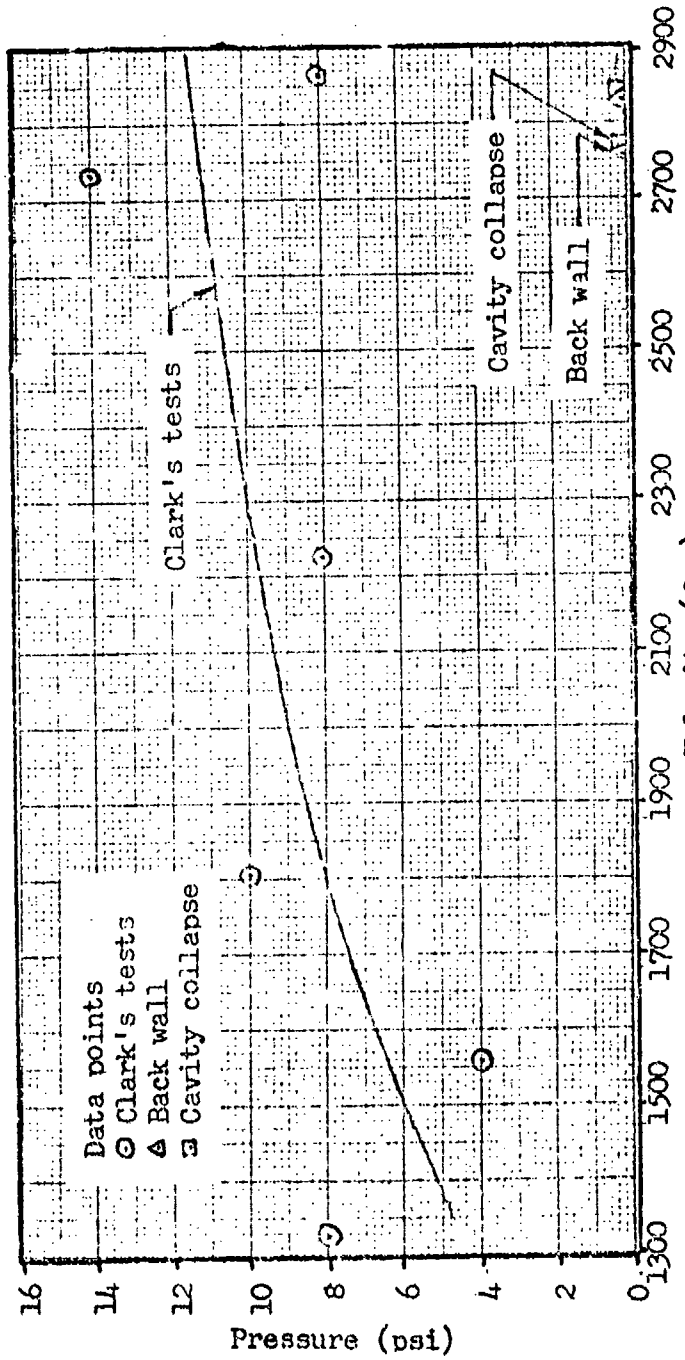

Figure 10, Impact Velocity vs Pressure
(Series 2, Spherical Projectiles)

General. Most of the analytical work performed on the hydraulic ram effect, Seaberg and Bristow (Ref 6) and Alverson (Ref 1) for example, has focused on the pressure wave generated by the projectile moving through the fluid. This was assumed to be the major contributor to massive fuel cell failures. Alverson (Ref 1) analyzed the hydraulic ram phenomenon by examining the kinetic energy of the projectiles. Shape was unimportant. The higher the kinetic energy of the projectile is, the higher the energy transferred to the fluid and the greater the damage to the tank. As a result, experiments have been conducted using high-velocity spherical projectiles. Spheres do not tumble as they pass through the fluid so the flight path can be fairly accurately estimated. A pressure wave was generated by the sphere passing through the fluid and the experimental data and the analytical results, such as those obtained by Clark (Ref 3), were in agreement. The cavity created behind the sphere was small and the pressure wave generated by the collapse of the cavity was significantly smaller than the original wave. Thus the second wave was neglected when fuel cell damage was analyzed. However, the tests conducted during this experiment showed that the pressure generated by the collapse of the cavity was approximately of the same magnitude as the first pressure wave generated by the projectile. The cavity collapse is also highly directional along the path of the projectile. As can be seen in Figures 11 and 12, the cavity following the projectile collapses not only inward but also along the projectile line-of-flight in the direction the projectile moved.

The results of this test suggest that when a full tank is struck by a high-velocity ogival projectile the following sequence of events takes place. The projectile passes through the tank creating two "small" holes; one on entry and one on exit. As the projectile moves through the tank it creates a large initial pressure wave in front of the projectile. This wave strikes the rear wall, but the wall can withstand the pressure because it is still intact. As the projectile moves through the fluid, it also creates a cavity behind the projectile. This cavity expands and then collapses, generating a pressure wave as large as the initial pressure wave. However, by this time the projectile has passed through the rear wall. There is a flaw in the wall and it is at this flaw that the cavity collapse pressure field is directed. And this is the point at which the massive damage is done to the tank. This sequence suggests a couple of areas

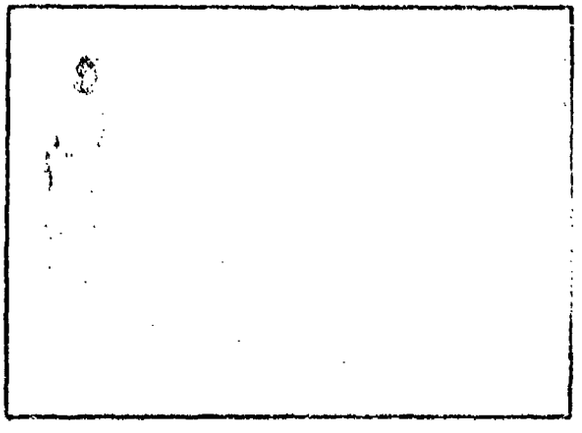

Figure 11, Cavity Created by Ogival Projectile

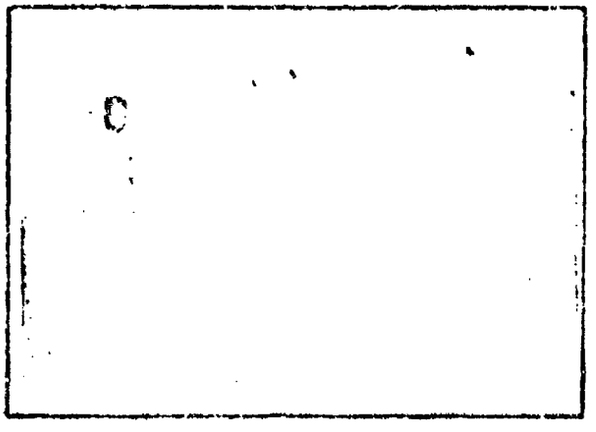

Figure 12, Collapse of Cavity Created by Ogival Projectile

in which future work could be performed. The ogival projectiles used in this study did not tumble until they were approximately ½ way through the tank (1 ft. from impact point). Since projectile tumbling is important to massive fuel cell damage, it would be desirable to have the projectile tumble as soon as possible. An investigation of the size, shape, and angle of impact for various projectiles and the effect of these variables on the initiation of tumbling could lead to development of projectiles with a higher kill rate than those presently used. Also, because tumbling is a factor, fuel cell geometry could play an important role in reducing massive damage. If a certain distance is required for a projectile to begin tumbling once it impacts a tank, fuel tanks could be designed such that this critical distance could never be obtained by a projectile.

V. Conclusions and Recommendations

Conclusions

1. While the data for this test was limited, it confirms Clark's tests with spheres and extends that work through the use of ogival projectiles.

2. A small amount of gas in a fuel-foam mixture significantly reduces the peak pressure measured at the back wall generated by the passage of the projectile through the fluid.

3. A small amount of gas in a fuel-foam mixture also either reduces the size of the cavity created by the passage of the projectile through the fluid, or reduces the pressure generated by the collapse of the cavity.

4. The use of spheres as projectiles in studying the hydraulic ram effect is ineffective because little if any cavity collapse pressure is generated.

5. The pressure field created by the collapse of the cavity created by the passage of the ogival projectile through the fluid is the major cause of massive full fuel cell damage.

Recommendations

1. Only ogival projectiles should be used in studying the attenuation of the hydraulic ram effect.

2. Tests should be conducted using thin walled fuel cells.

3. A foam should be designed which will combine the shock attenuation effects of a gas-filled fiber with the flame suppressing characteristics of reticulated polyurethane foam.

Bibliography

1. Alverson, R. et al. "Shock Effects in Fuel Cells." SRI Report PGD-7708. Menlo Park, California: Stanford Research Institute, (January 1970).

2. Bristow, R. J. "Design of Hydraulic Ram Resistant Structure." Paper 10-11, Seattle, Washington: The Boeing Company, (1971).

3. Clark, J. W. "An Experimental Study of Attenuation of Shock Waves in Three Mixtures." M.S. Thesis, Wright-Patterson Air Force Base, Ohio: Air Force Institute of Technology, (June 1972).

4. Lavery, B. Personal correspondence to John R. Breuninger, Jr., (January 1973).

5. Northrop Corporation. "Analysis of Hydrodynamics of Projectiles Fired into Fuel Tanks." Technical Brief NB70-247. Hawthorne, California: Aircraft Division, Northrop Corporation, (January 1971).

6. Seaberg, C. T. and R. Bristow. "Fuel Tank Impact." FADS-37. Seattle, Washington: The Boeing Company, (January 1967).

7. Stepka, F. S., et al. "Investigation of Characteristics of Pressure Waves Generated in Water Filled Tanks Impacted by High-Velocity Projectiles." NASA TN D-3143, Washington: National Aeronautics and Space Administration, (December 1965).

8. Torvik, P. J. and J. W. Clark. "The Reduction of Impact Induced Pressures in Fuel Tanks." Unpublished Report.

9. US Air Force Flight Dynamics Laboratory. "Hydraulic Ram Study." AFFDL Project 43630109. Unpublished Report.

10. US Department of Housing and Urban Development. "Carpet Cushion." Materials Release No. 768. Washington: HUD, (June 1972).

11. Winters, D. W. "Dynamic Response of Water to Ballistic Impact." MS Thesis, Wright-Patterson Air Force Base, Ohio: Air Force Institute of Technology, (June 1970).

Appendix A

Pneumacel

Pneumacel, shown in Figure 26, is a Du Pont product presently manufactured commercially as a carpet padding. The term "pneumacel" is not a trademark; it is a generic designation for materials made of permanently pressurized cellular fibers. The word "pneumacel" is defined as: A resilient, pneumatic, strand, sheet, or cushion composed of a cellular polymer structure having predominantly closed cells that are inflated to higher than surrounding pressure with two or more gases, one of which is essentially impermeable to the cell walls (Ref 10).

A supply of Du Pont Pneumacel, Lansdowne Model 5000, was made available for this study by Dr. Bernard Lavery, Christina Laboratory, Du Pont Corp., Wilmington, Delaware, 19898. The following information was also provided by Dr. Lavery (Ref 4).

Mat Characteristics

Randomly oriented, thermoplastically bonded Pneumacel fibers.

Density: approximately 1.5 lb/cu ft.

Thickness: approximately 0.475 in.

Fiber Characteristics

Small, uniform, polyhedral cells (Fig 27).

Thin, highly oriented cell walls.

Chemical properties: "Dacron" polyester fiber inflated with a fluorinated hydrocarbon blowing agent.

Density: approximately 0.023 gm/cu cm, 12% of the weight is inflatent.

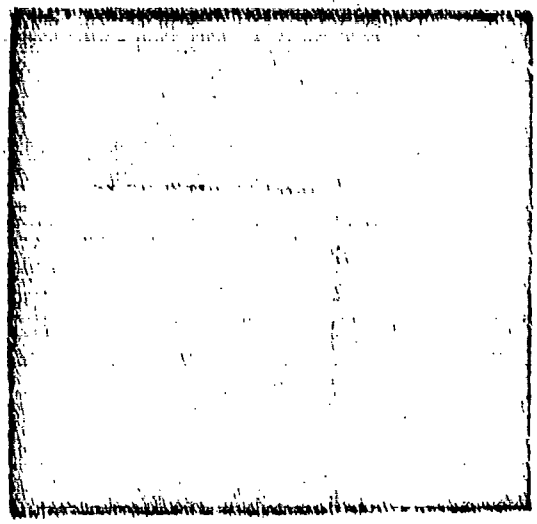

Figure 13
Pneumacel

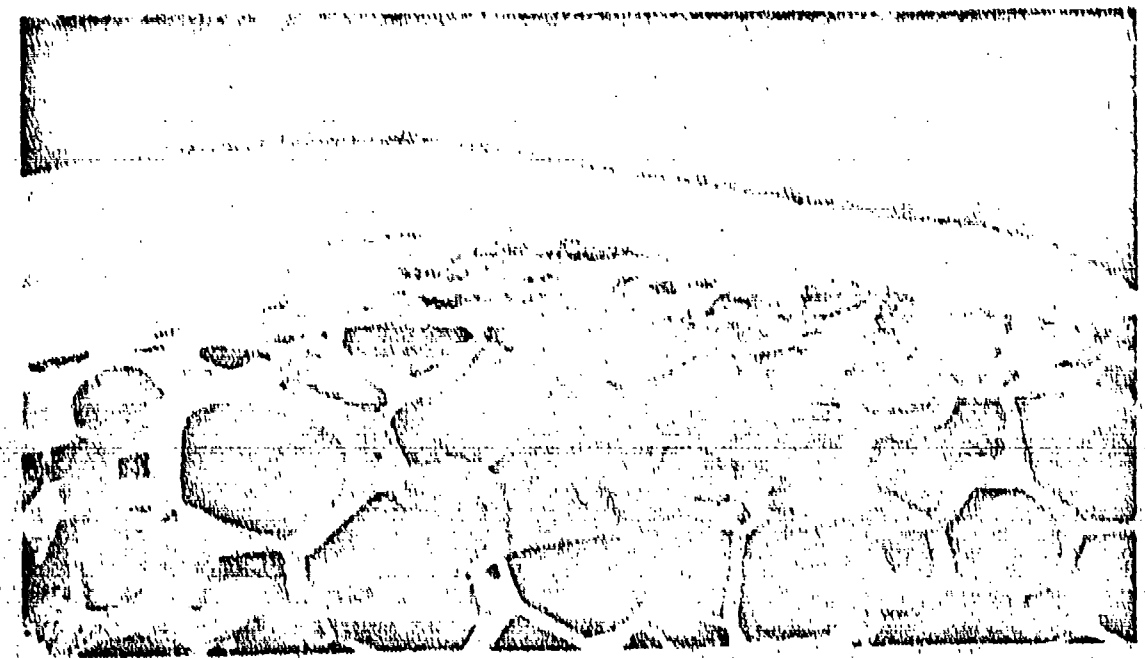

Figure 14
Cross-section photomicrograph of Pneumacel
(magnified 4000 times)

Appendix B

Blow Out Plugs

Four blow out plugs were placed in the back wall of the target tank in an attempt to determine if the momentum of the plugs after being blown out could be related to the strength of the driving force, a shock wave in this case. If a relationship could be determined, this technique could then be used in future tests. Rather than placing expensive pressure transducers near the expected projectile impact point with a good chance of the transducer being struck and destroyed, the blow out plugs could be used to determine the shock strength.

The plugs were constructed of 2024 aluminum to reduce the mass. They were constructed in the shape of truncated cones so that if they rolled on exit there would be no binding. Two velocity screens were used to measure the plug's velocity. High speed photography would have been preferable to determine plug velocity, but it was unavailable at the time due to priority mission requirements.

Initially, the plugs were placed in the back plate and were sealed with zinc chromate. In order to hold the plug in place, a strip of masking tape was placed over the plug end. This procedure was unacceptable because the seal was poor and the tape held the plug so firmly in place nothing was happening.

The plugs were then sealed with a film of aircraft grease. The grease provided a watertight seal and enough surface tension to hold the plugs in place against the water static pressure head. However, when the shock hit the plug, it was blown out as desired.

Velocity data on the plugs was obtained only during the last 4 shots in Series 1. The four velocities were: 29 fps, 82 fps, 236 fps, 187 fps. During shot 15 when the 236 fps velocity was recorded it was later determined that the projectile had lodged sidewise across the hole in the back plate in which the blow out plug had been resting. Thus it was a little more than a shock wave that drove the plug out of the hole.

To determine the force the following equations were used:

$$V^2 = 2 a S$$

and

$$P = \frac{M a}{A}$$

where V is plug velocity

S is distance plug moved while force was applied (3/4 in.)

M is plug mass (405 grains)

A is surface area over which the pressure acts (1/16π sq. in.)

Using, $P = \frac{M V^2}{2AS}$

the pressures determined for the various plug velocities were:

Table III

Computed and Actual Pressure
During Blow Out Plug Test

Shot No.	Velocity	Computed Pressure (psi)	Actual Pressure (psi)
13	29	60	150
14	82	482	630
15	236	3996	590
16	187	2509	800

The data appears close to the actual value in some cases and completely wrong in others. This is due to the fact that if the projectile hits on, or very close to, the plug it is not only the pressure wave that drives out the plug but also the actual impact of the projectile. This test resulted in little usable data.

If the velocity of the plugs could be determined from high speed photography, more accurate data should be obtained. A plug could be selected on the film which was not near the impact point and was thus accelerated simply by the pressure wave. Further study of this data gathering method should be accomplished.

Appendix C

Oscilloscope Pictures

The Polaroid photographs of the pressure traces for all successful tests follow. Figures 15 - 27 are for series 1 (water only) and Figures 28 - 37 are for series 2 (water/Pneumacel).

All traces run from left to right. Positive pressure is read below the zero reference line. The time reference is from the passage of the projectile through the triggering screen located 2 in. in front of the tank. One large division on a photograph is equal to 1 cm. Gages 1 and 2 were located inside the tank. Gages 3, 4, 5, and 6 were located in the back wall of the tank near the projectile impact point.

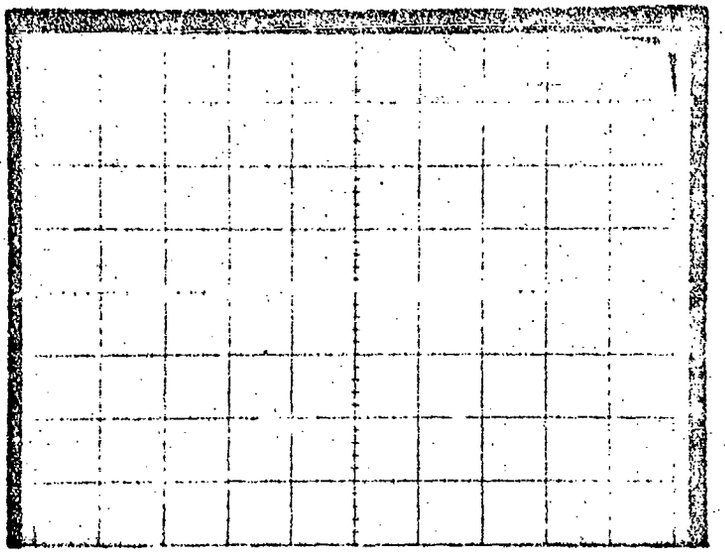

Shot 1

Water

Gages 1 & 2, 5 msec/cm
200 psi/cm

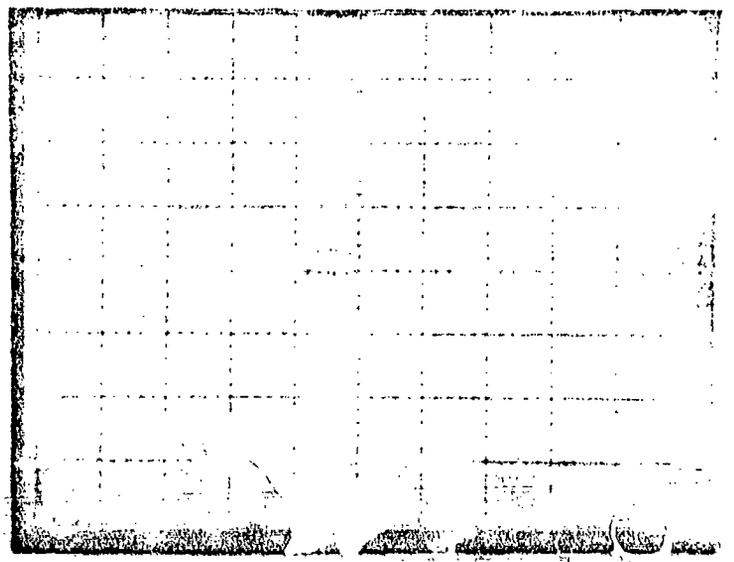

Gages 3 & 4, 2 msec/cm
200 psi/cm

Projectile velocity-
1000 fps

Figure 15
Scope picture, Series 1, Part 1, Shot 1

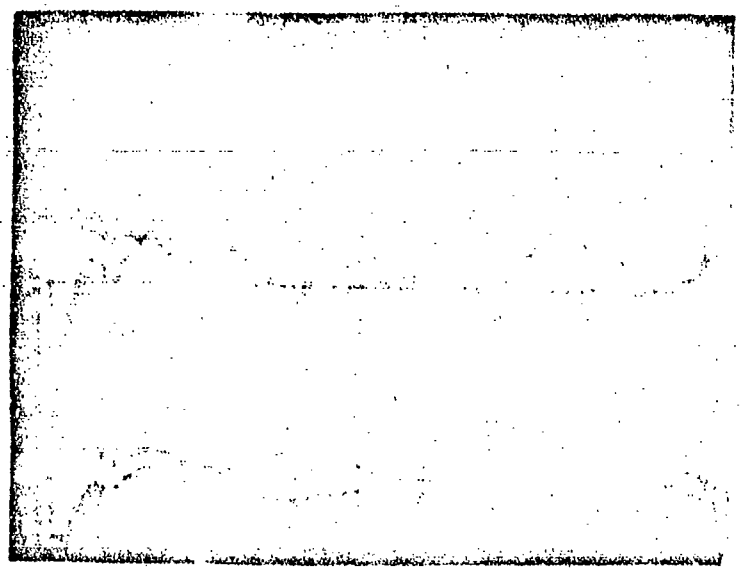

Shot 3

Water

Gages 1 & 2, 5 msec
20 psi

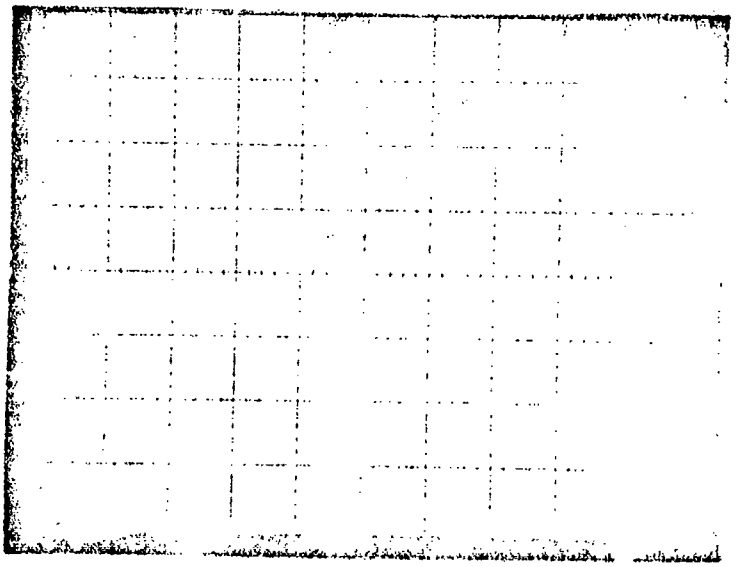

Gages 3 & 4, 1 msec
20 psi

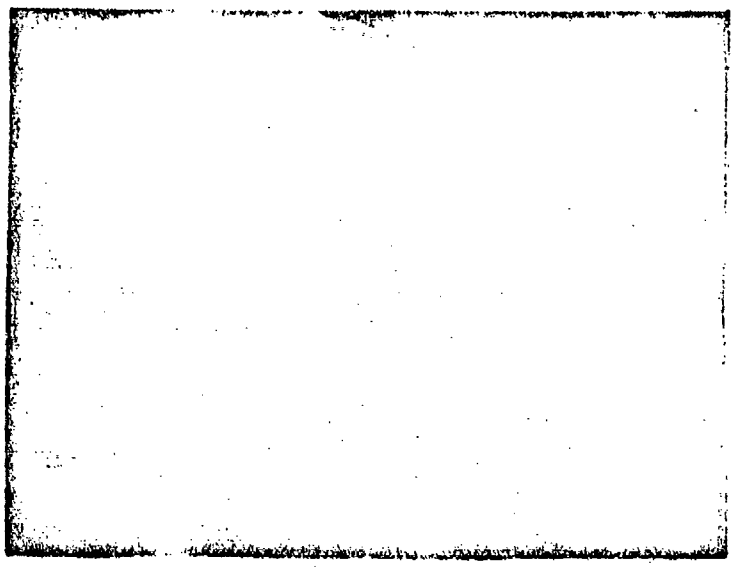

Gages 5 & 6, 1 msec
20 psi

Projectile velocity
1700 fps

Figure 16
Scope picture, Series 1, Part 1, Shot 3

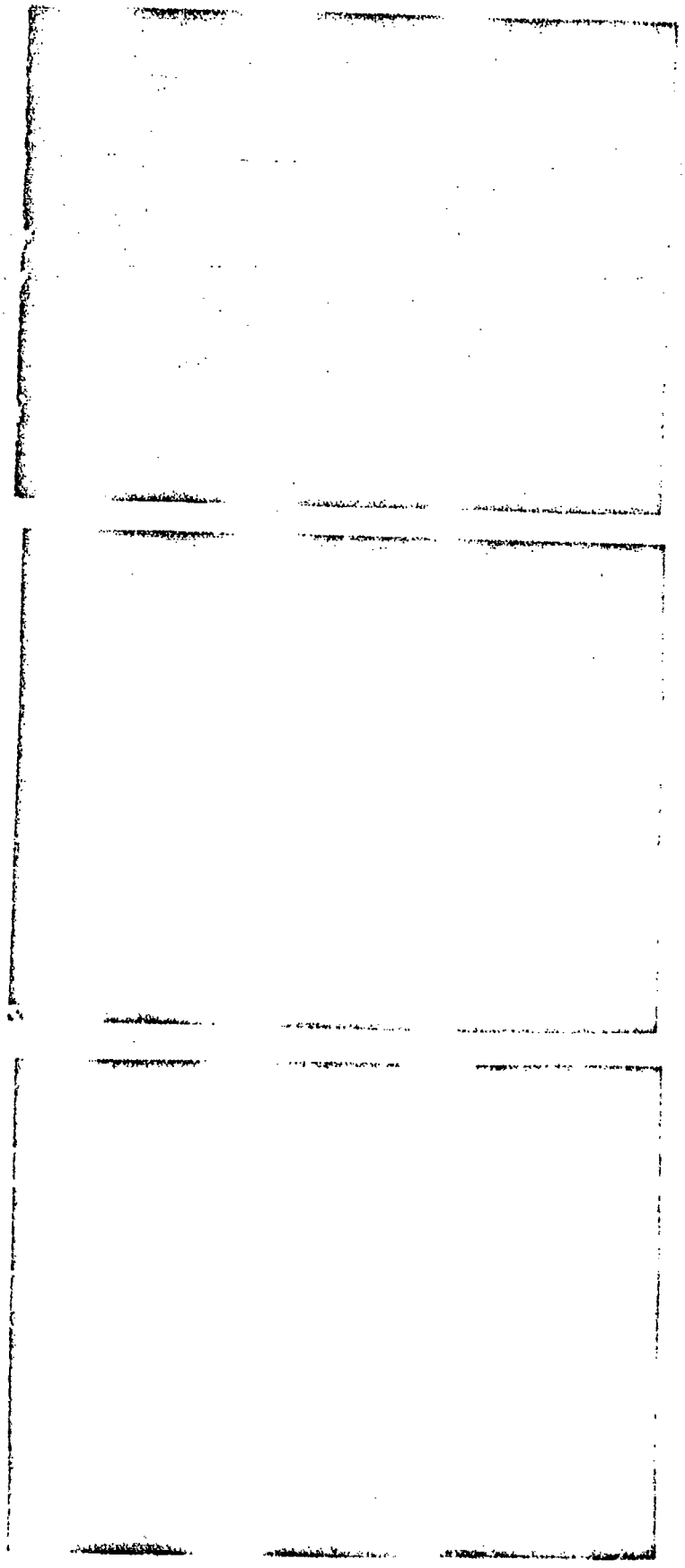

Gages 1 & , 5 msec/cm
100 psi/cm

Gages 3 & , 0.5 msec/cm
100 psi/cm

Gages 5 & , 0.5 msec/cm
100 psi/cm

Projectil velocity-
139 fps

gure 17
e picture, ries 1, Pa 1, Shot 5

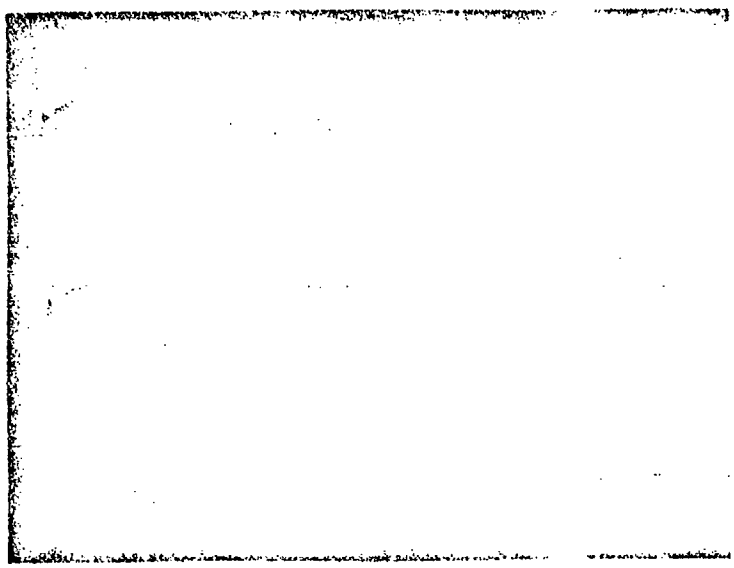

Shot 6

Water

Gages 1 & 2, 5 msec/cm
100 psi/cm

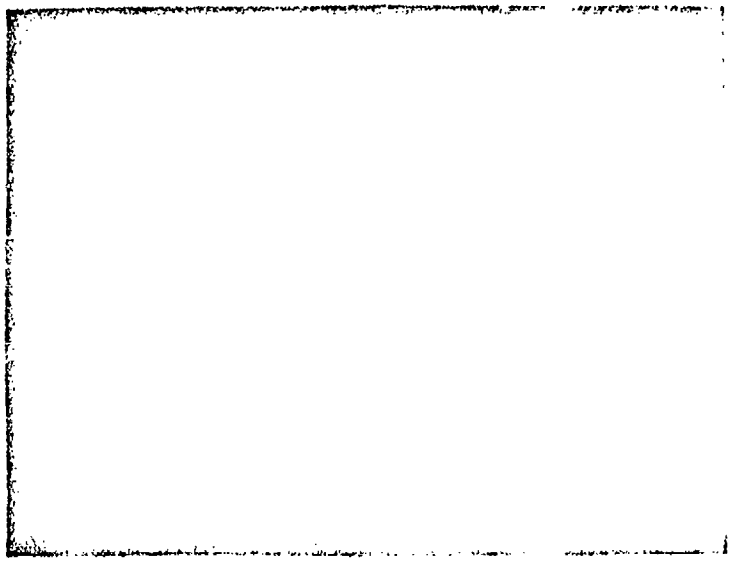

Gages 3 & 4, 0.5 msec/cm
100 psi/cm

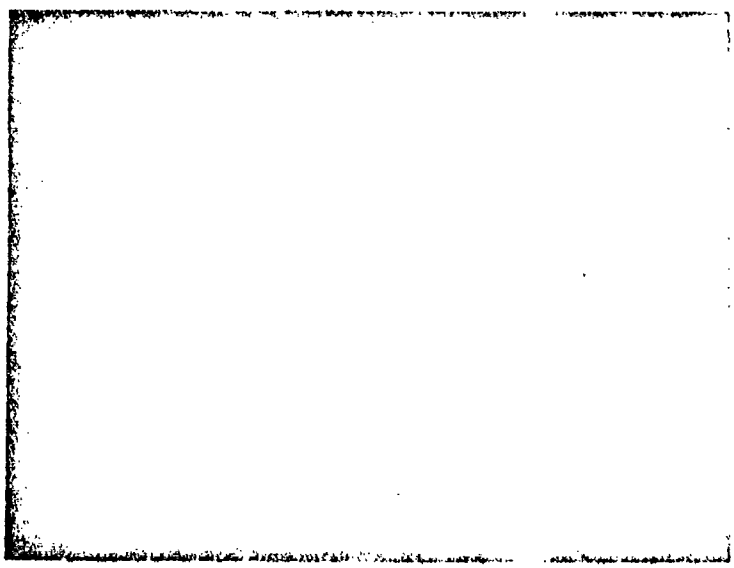

Gages 5 & 6, 0.5 msec/cm
100 psi/cm

Projectile velocity-
1406 fps

Figure 18
Scope picture, Series 1, Part 1, Shot 6

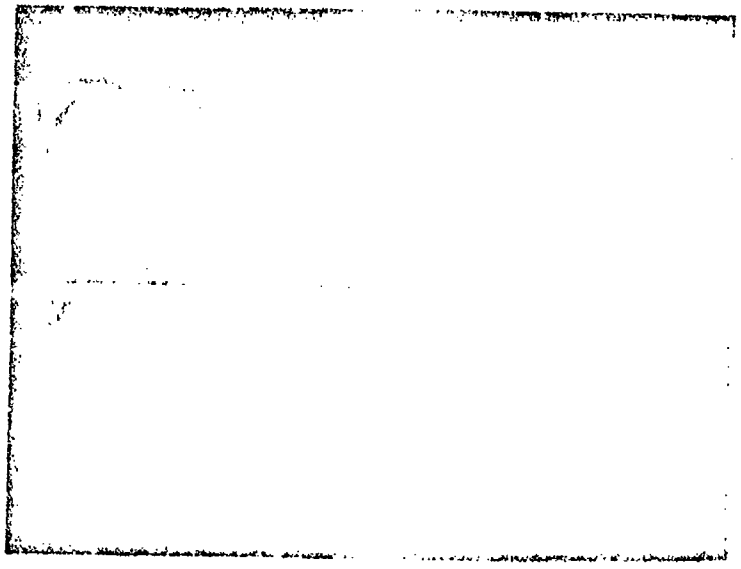

Sh /

wa

ges 1 & 2 msec/cm

) psi/cm

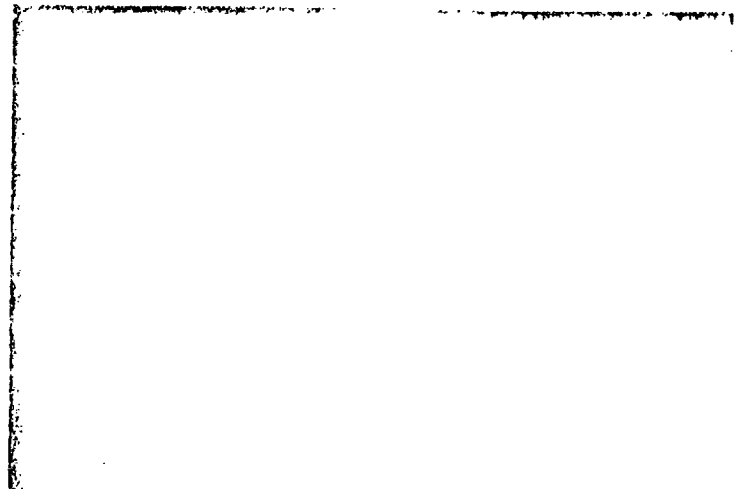

ges 3 & 4 .5 msec/cm

00 psi/cm

ges 5 & 0 .0 DATA

rojectile locity-

2037

Fig. 19

Scope picture, Ser. 1, Part 1, Shot 7

Oscilloscope Traces for Shot 8

can be found on Page 17.

Figure 20

Scope picture, Series 1, Part 1, Shot 9

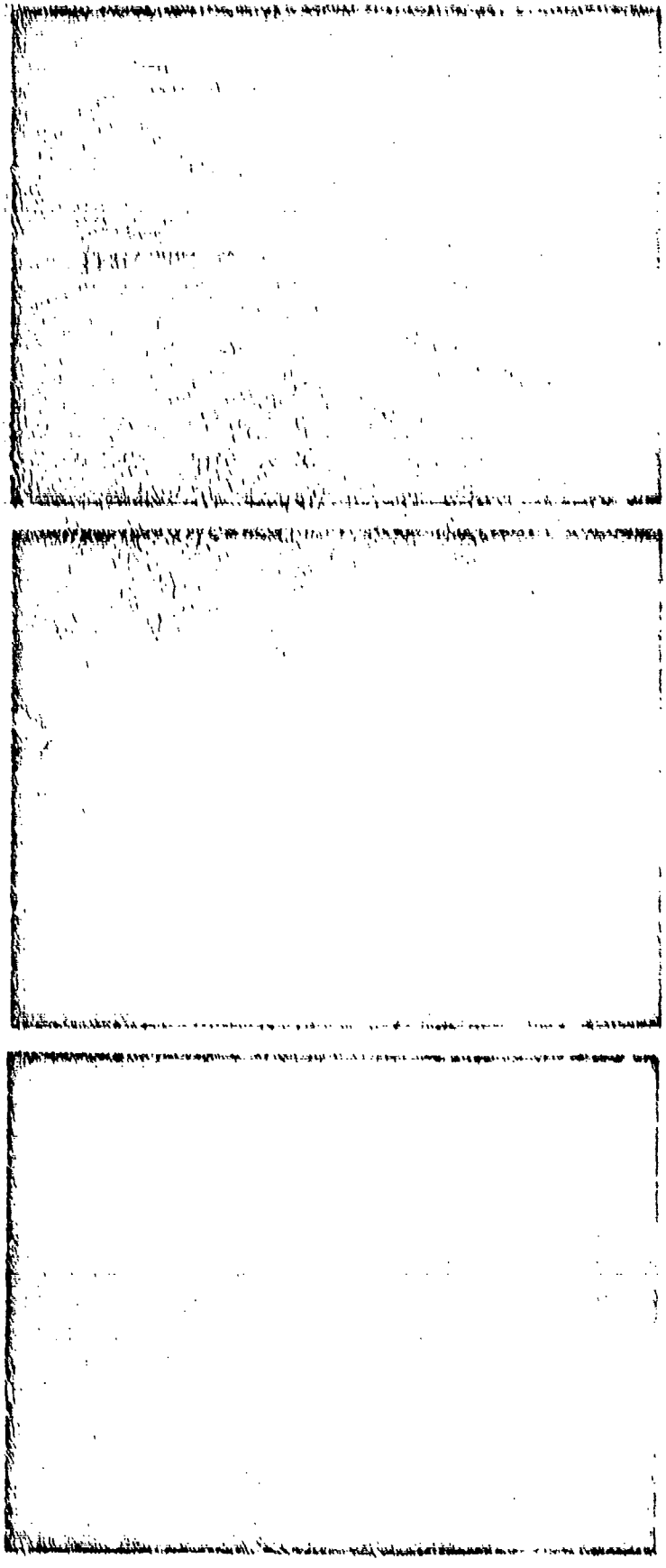

Shot 10

Water

Gages 1 & 2, 2 msec/cm
100 psi/cm

Gages 3 & 4, 0.5 msec/cm
100 psi/cm

Gages 5 & 6, 0.5 msec/cm
100 psi/cm

Projectile velocity-
2739 fps

Figure 21.
Scope picture, Series 1, Part 1, Shot 10

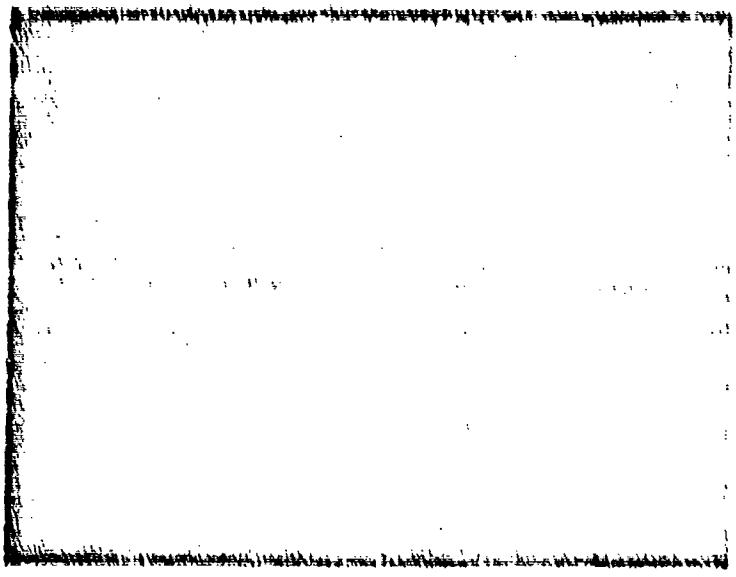

Shot 11

Water

Gages 1 & 2, 2 msec/cm
100 psi/cm

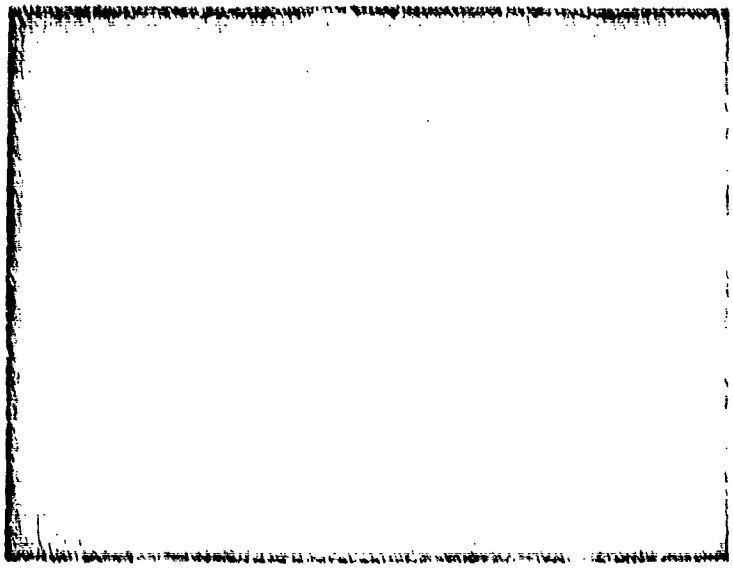

Gages 3 & 4, 0.5 msec/cm
100 psi/cm

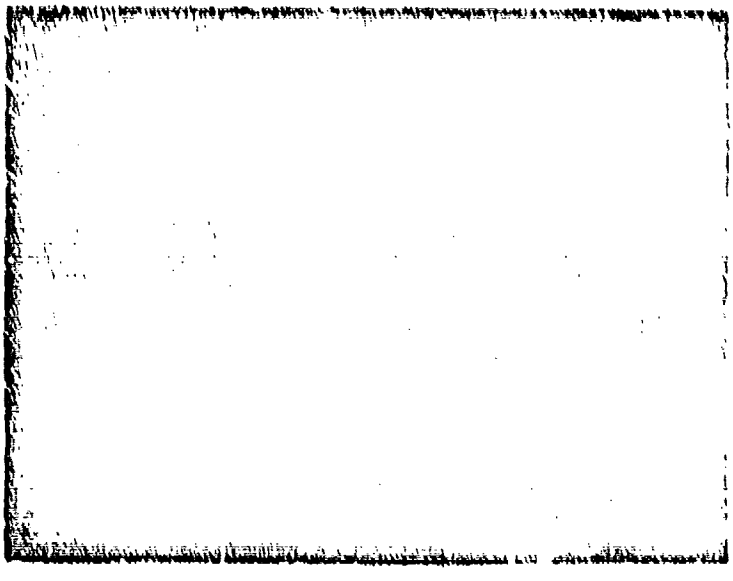

Gages 5 & 6, 0.5 msec/cm
100 psi/cm

Projectile velocity-
2928 fps

Figure 22
Scope picture, Series 1, Part 1, Shot 11

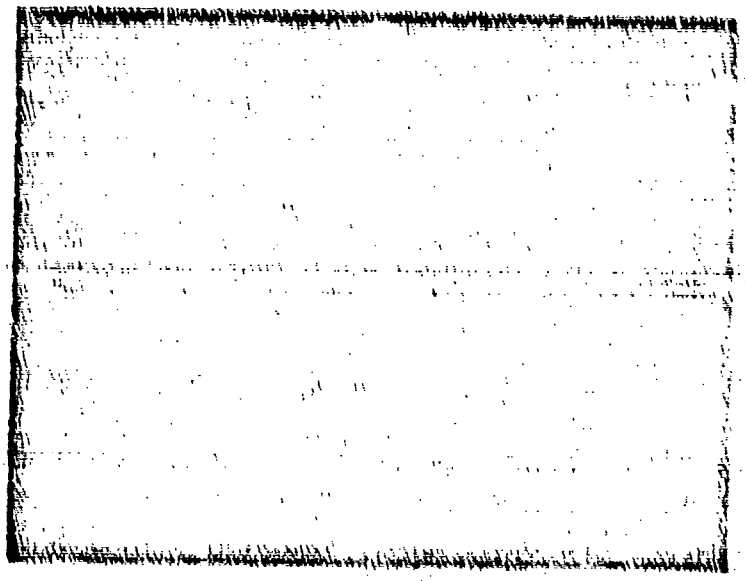

Shot 12

Water

Gages 1 & 2, 2 msec/cm
100 psi/cm

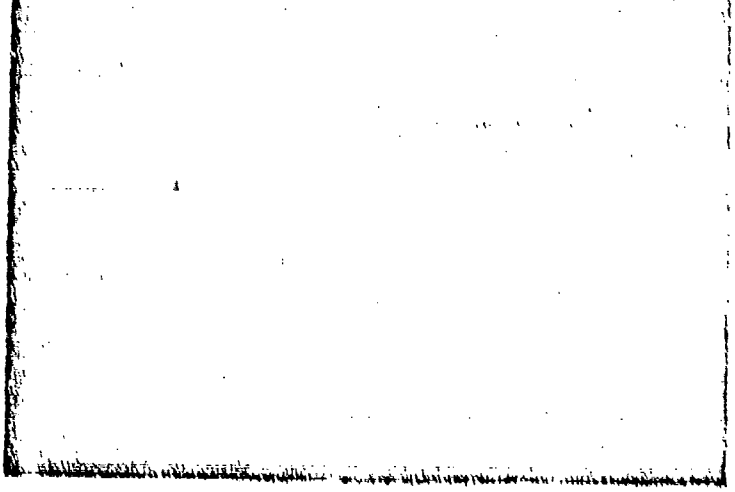

Gages 3 & 4, 0.5 msec/cm
100 psi/cm

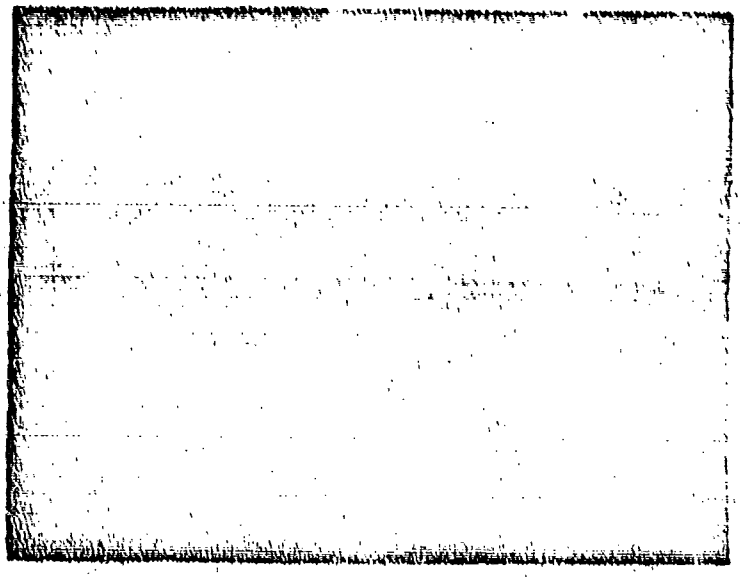

Gages 5 & 6, 0.5 msec/cm
100 psi/cm

Projectile velocity-
2928 fps

Figure 23
Scope picture, Series 1, Part 1, Shot 12

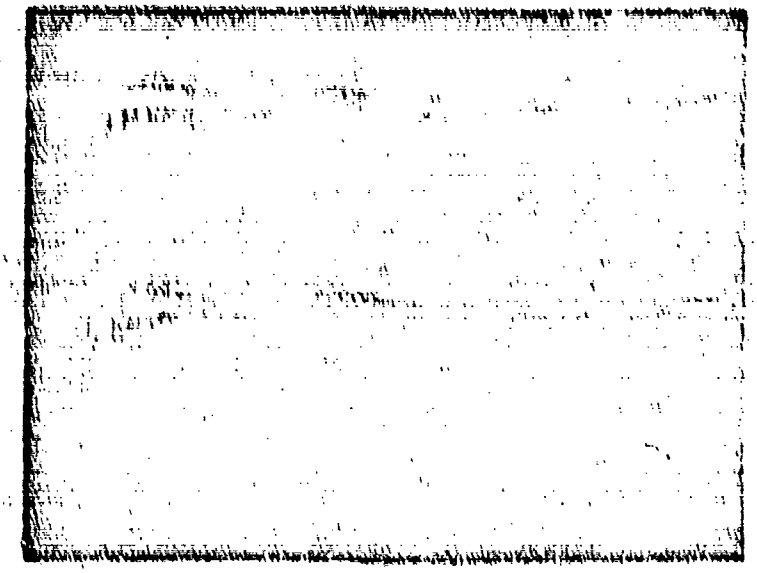

Shot 13

Water

Gages 1 & 2, 2 msec/cm
100 psi/cm

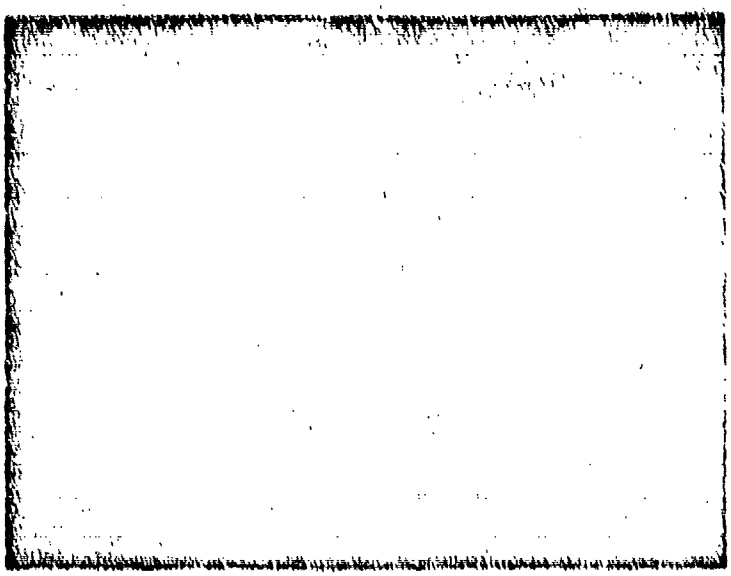

Gages 3 & 4, 0.5 msec/cm
100 psi/cm

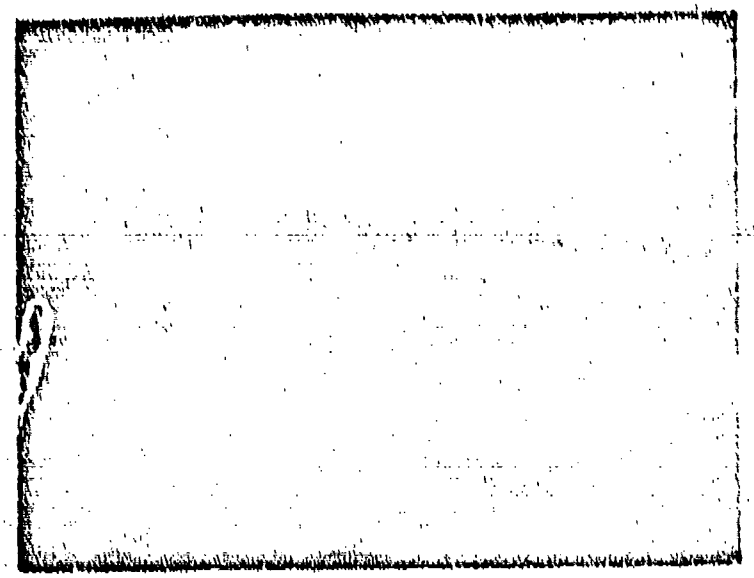

Gages 5 & 6, 0.5 msec/cm
100 psi/cm

Projectile velocity-
3091 fps

Figure 24
Scope picture, Series 1, Part 1, Shot 13

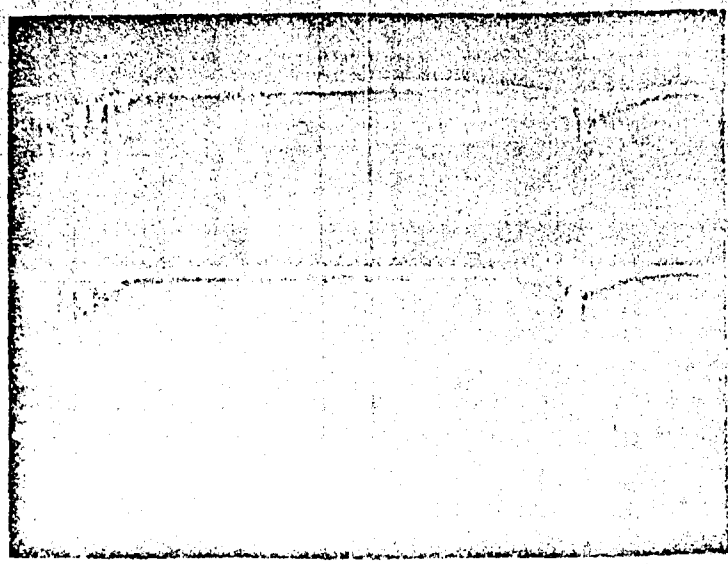

Shot 14

Water

Gages 1 & 2, 2 msec/cm
200 psi/cm

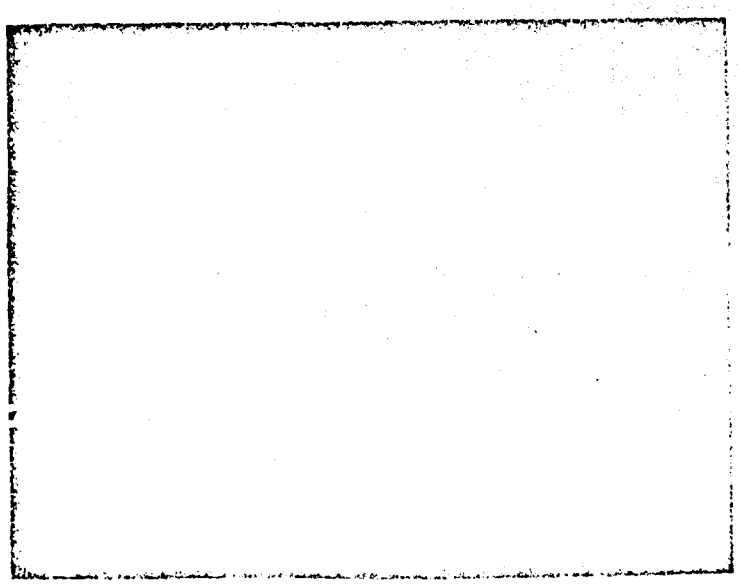

Gages 3 & 4, 0.5 msec/cm
200 psi/cm

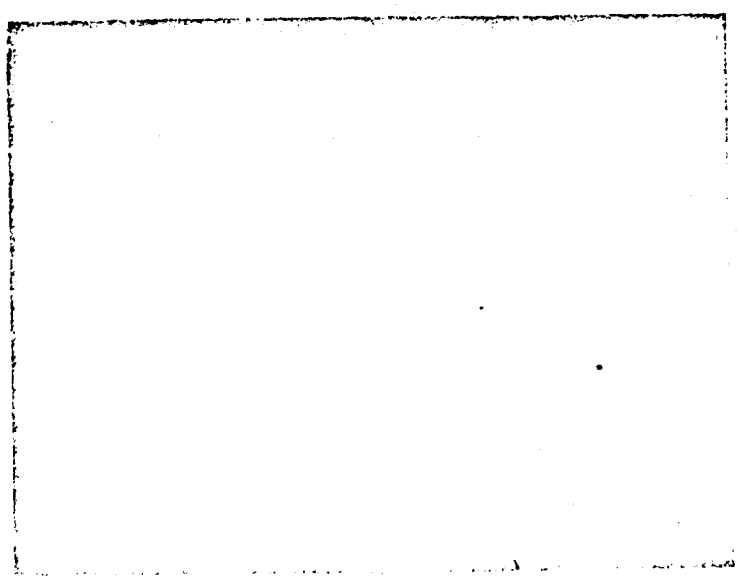

Gages 5 & 6, 0.5 msec/cm
200 psi/cm

Projectile velocity-
2770 fps

Figure 25

Scope picture, Series 1, Part 2, Shot 14

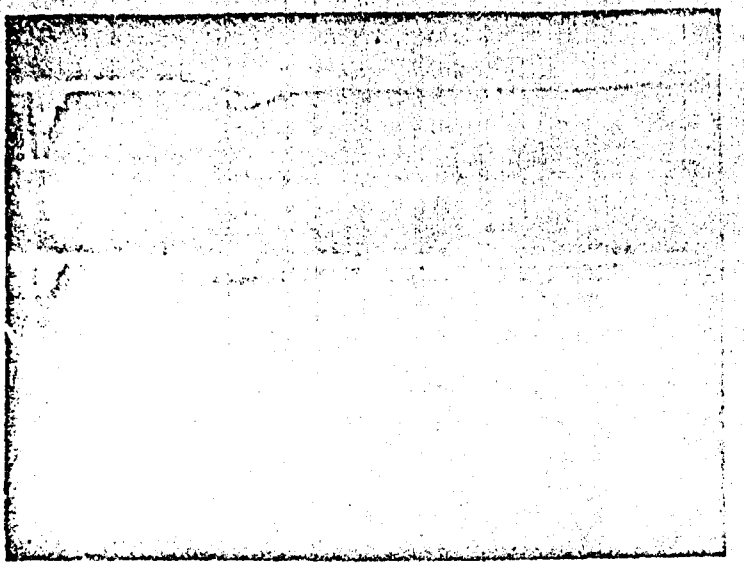

Shot 15

Water

Gages 1 & 2, 5 msec/cm
200 psi/cm

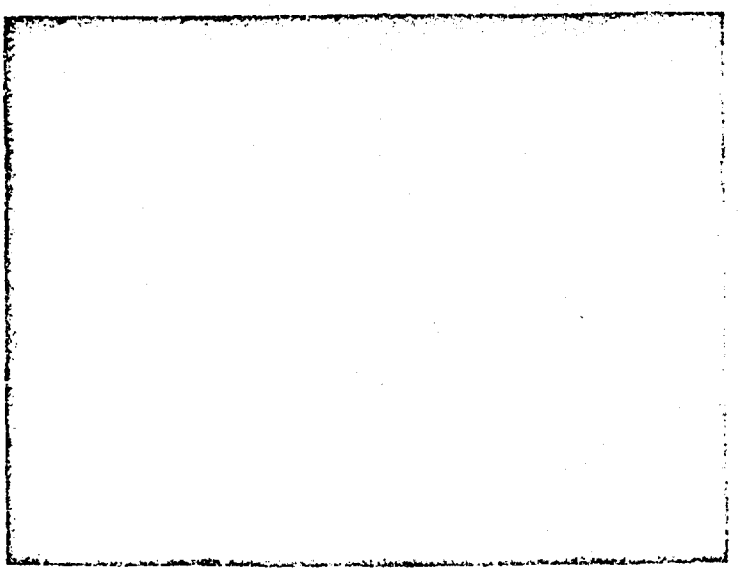

Gages 3 & 4, 0.5 msec/cm
200 psi/cm

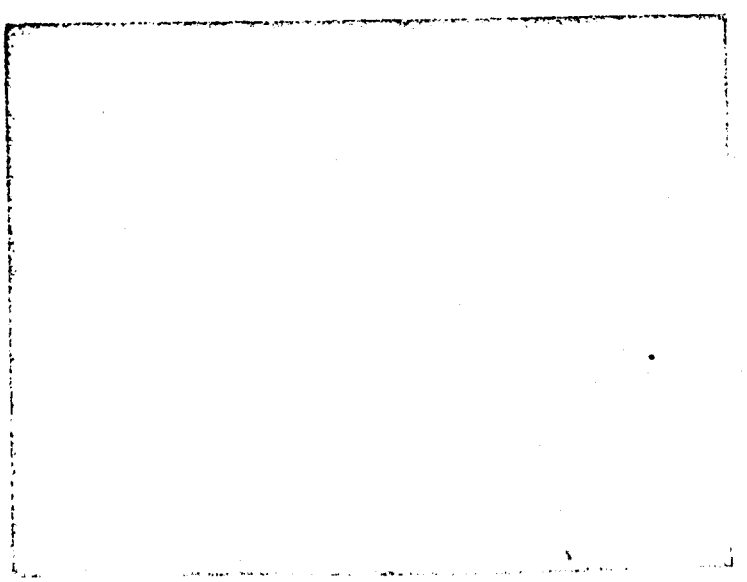

Gages 5 & 6, 0.5 msec/cm
200 psi/cm

Projectile velocity-
2691 fps

Figure 26

Scope picture, Series 1, Part 2, Shot 15

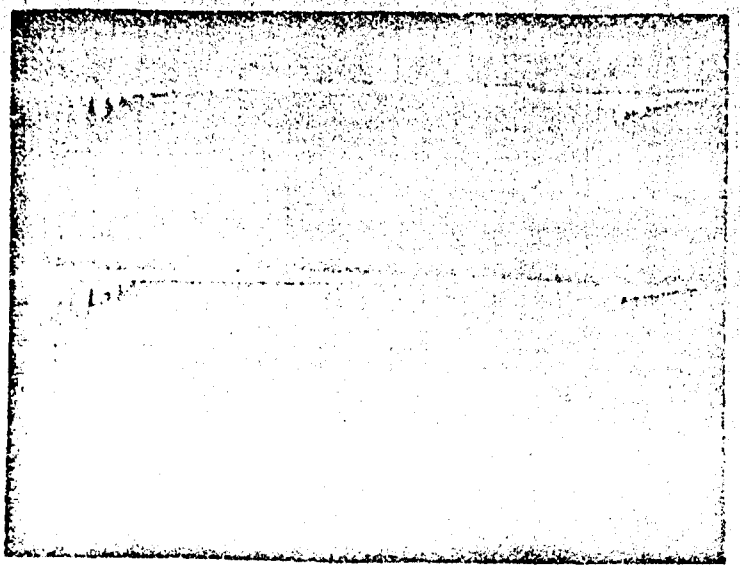

Shot 16

Water

Gages 1 & 2, 2 msec/cm
200 psi/cm

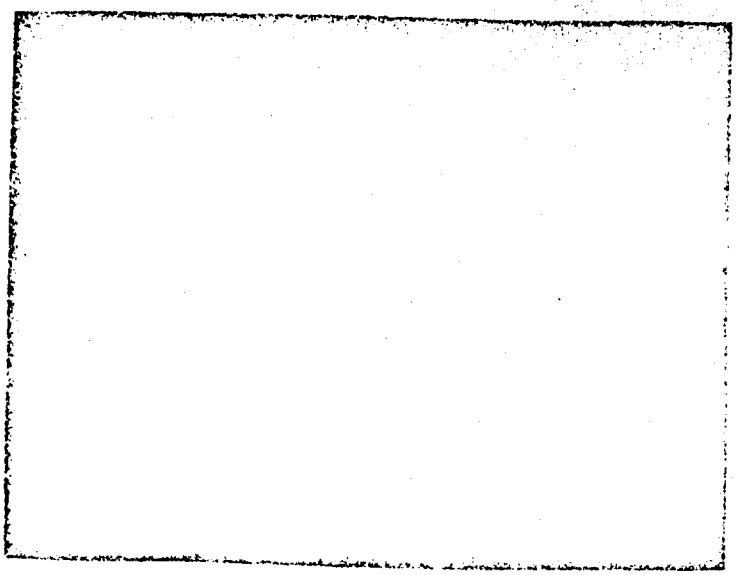

Gages 3 & 4, 0.5 msec/cm
200 psi/cm

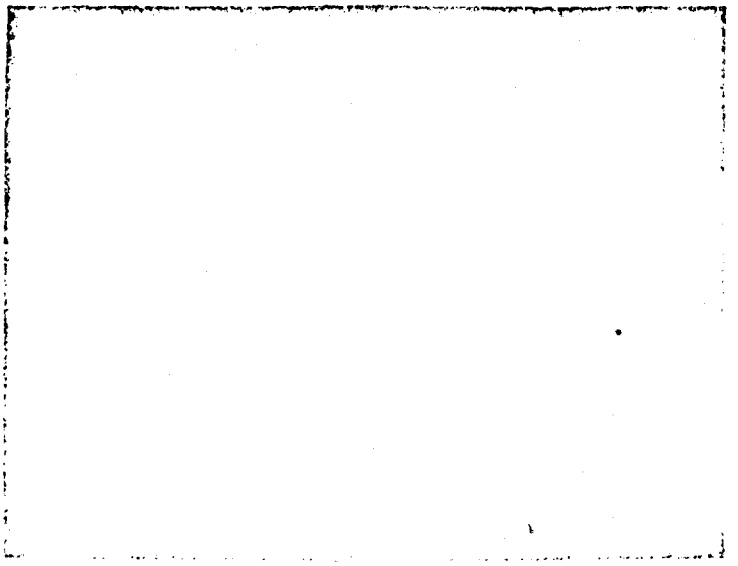

Gages 5 & 6, 0.5 msec/cm
200 psi/cm

Projectile velocity-
2680 fps

Figure 27

Scope picture, Series 1, Part 2, Shot 16

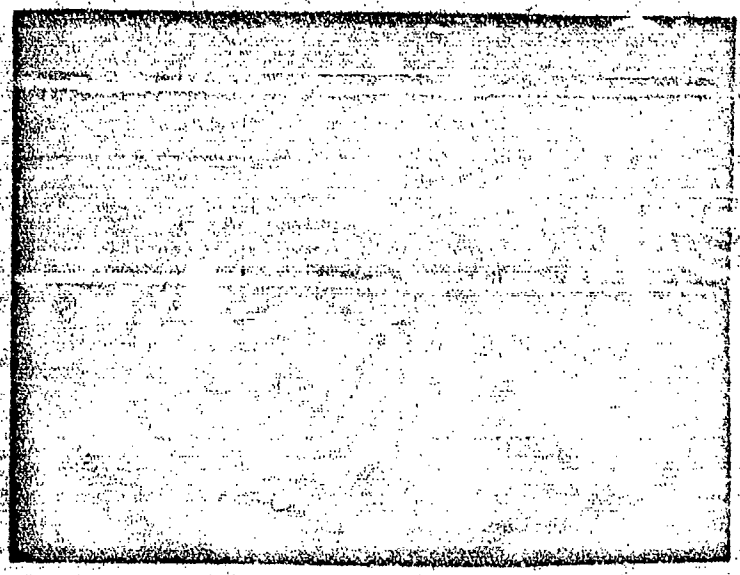

Shot 1A

Pneumatic

Gages 1 & 2, 2 msec/cm
100 psi/cm

Gages 3 & 4, 0.5 msec/cm
100 psi/cm

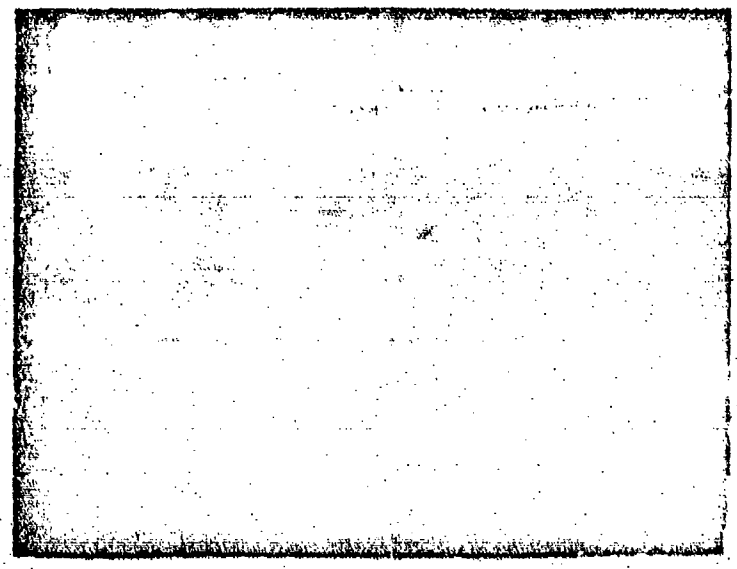

Gages 5 & 6, 0.5 msec/cm
100 psi/cm

Projectile velocity-
2750 fps

Figure 28
Scope picture, Series 2, Part 1, Shot 1A

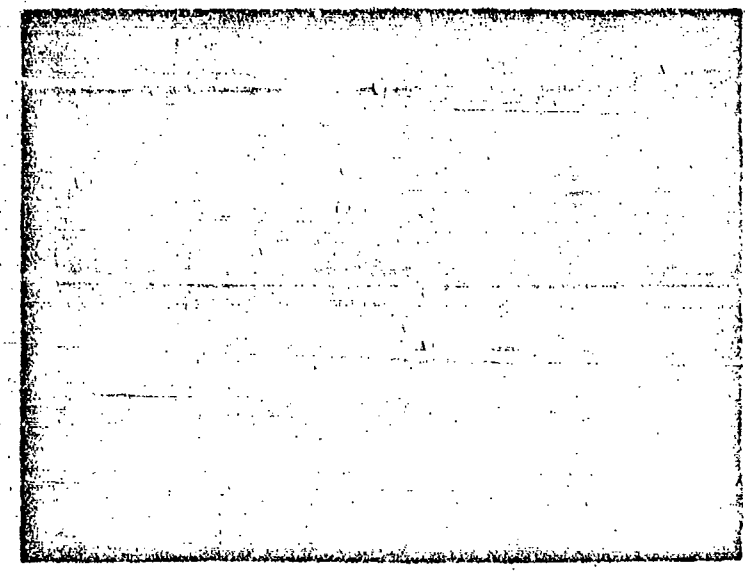

Shot 2A

Pneumacel

Gages 1 & 2, 2 msec/cm
100 psi/cm

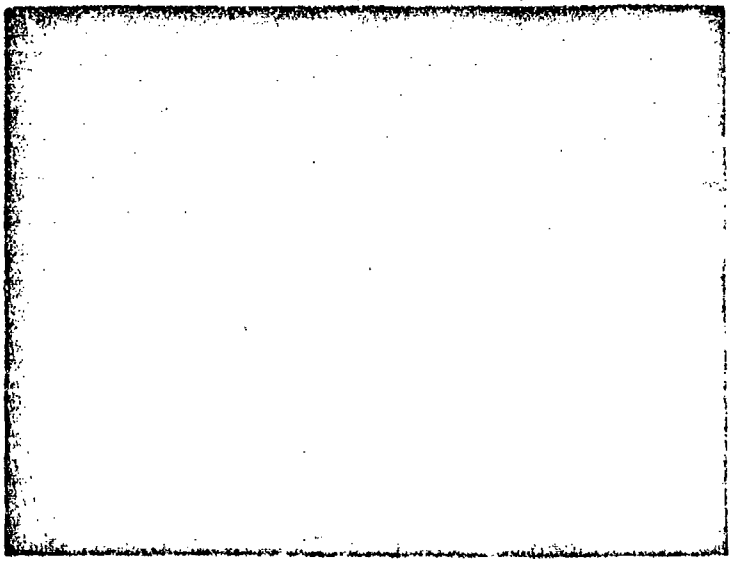

Gages 3 & 4, 0.5 msec/cm
100 psi/cm

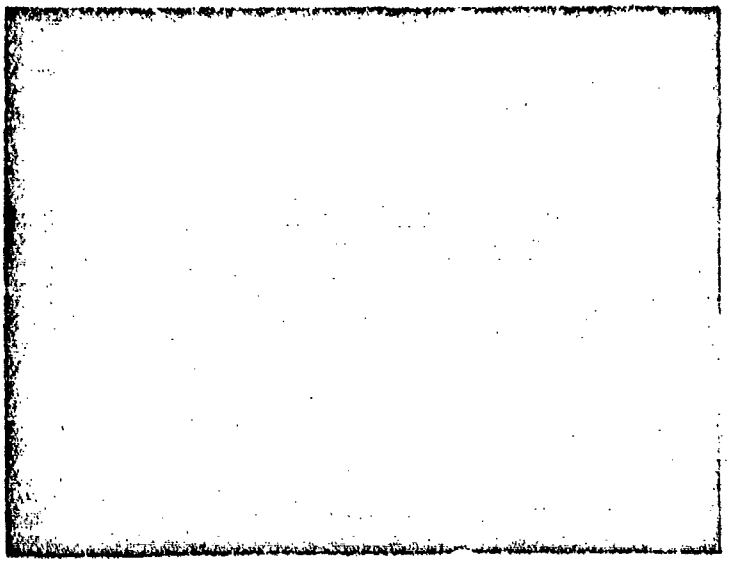

Gages 5 & 6, 0.5 msec/cm
100 psi/cm

Projectile velocity-
2750 fps

Figure 29
Scope picture, Series 2, Part 1, Shot 2A

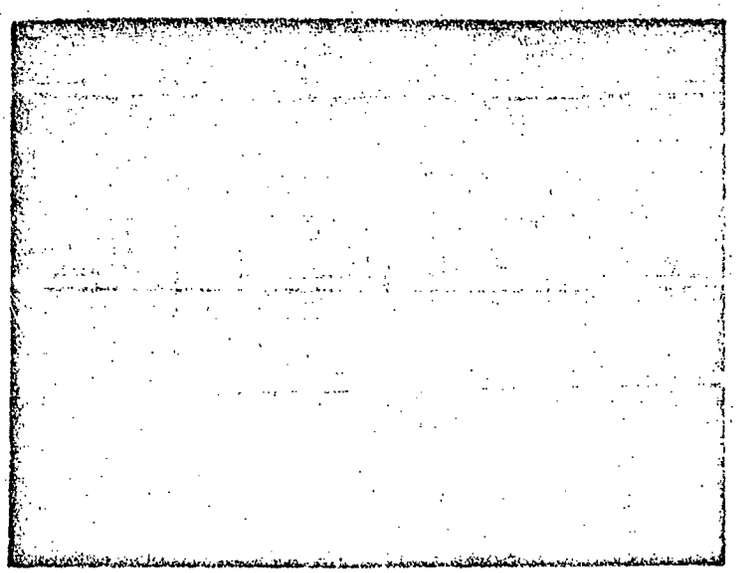

Shot 3A

Pneumacel

Gages 1 & 2, 2 msec/cm
100 psi/cm

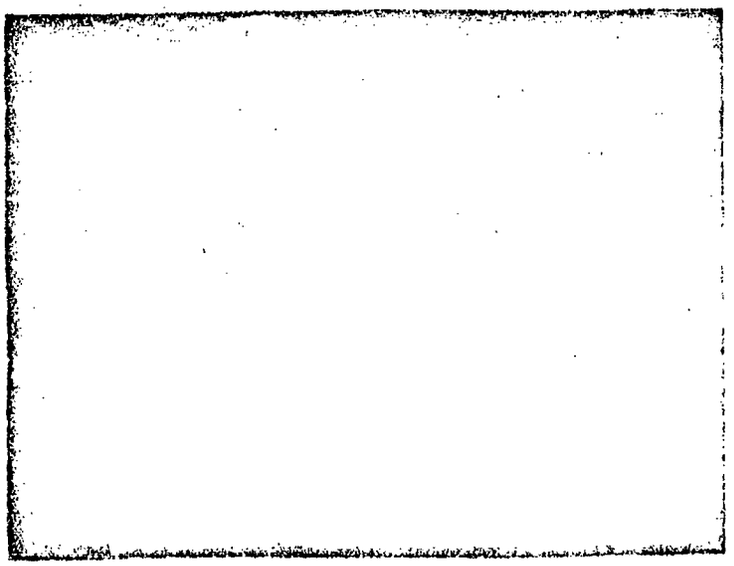

Gages 3 & 4, 0.5 msec/cm
100 psi/cm

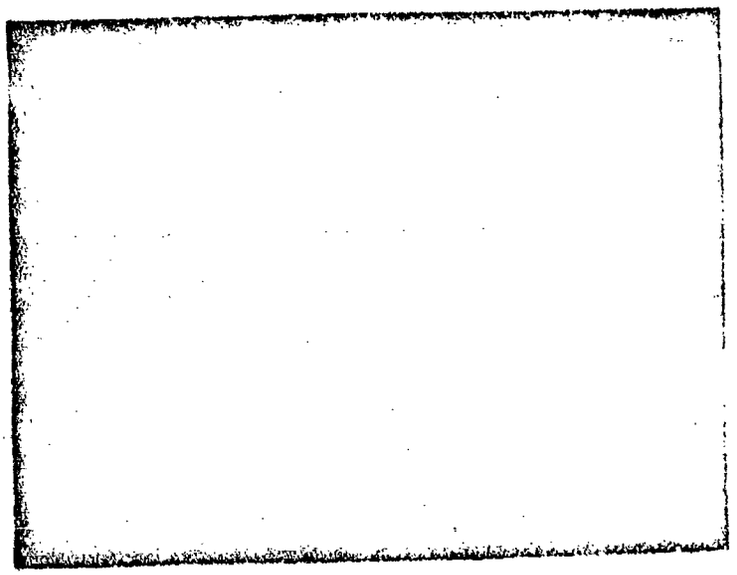

Gages 5 & 6, 0.5 msec/cm
100 psi/cm

Projectile velocity-
2750 fps

Figure 30
Scope picture, Series 2, Part 1, Shot 3A

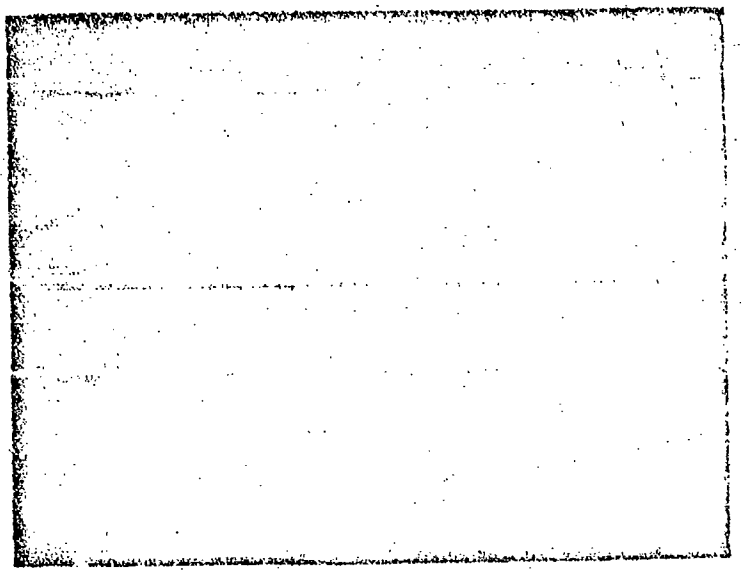

Shot 4A

Pneumacel

Gages 1 & 2, 2 msec/cm
100 psi/cm

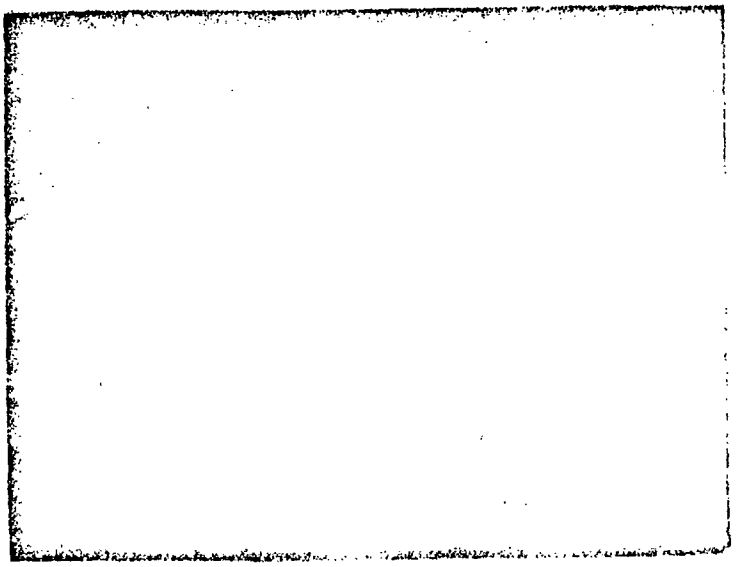

Gages 3 & 4, 0.5 msec/cm
100 psi/cm

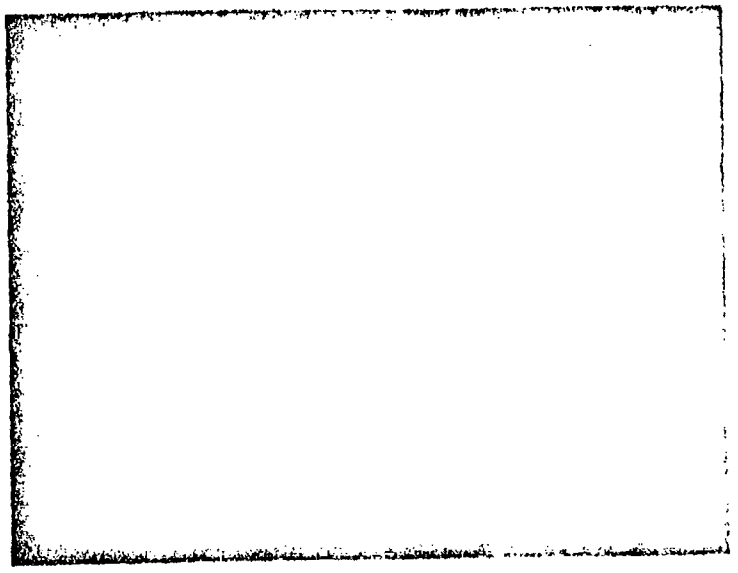

Gages 5 & 6, 0.5 msec/cm
100 psi/cm

Projectile velocity-
2750 fps

Figure 31
Scope picture, Series 2, Part 1, Shot 4A

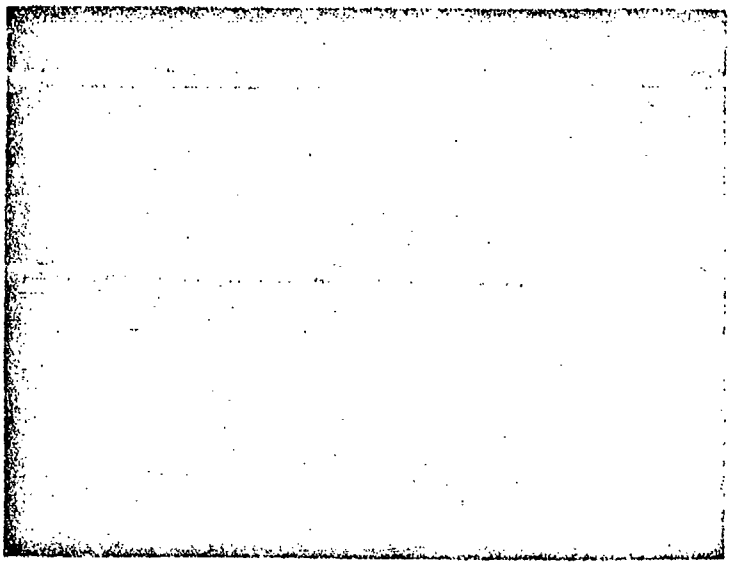

Shot 5A

Pneumacel

Gages 1 & 2, 2 msec/cm
100 psi/cm

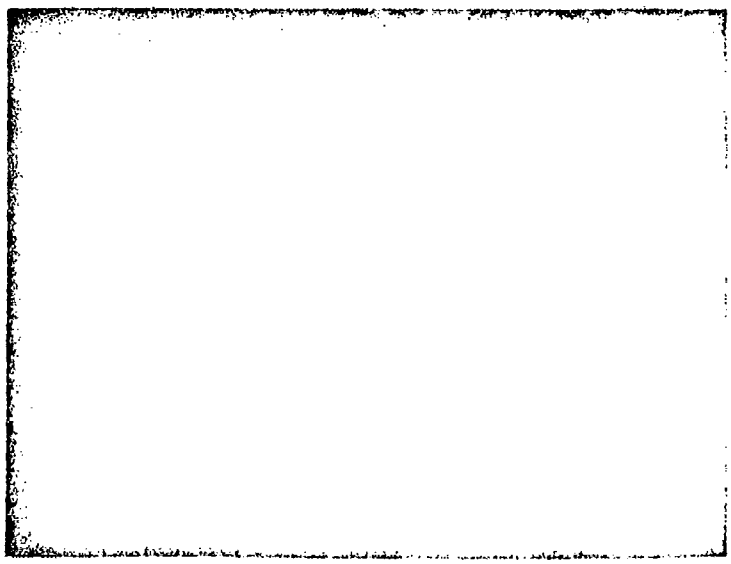

Gages 3 & 4, 0.5 msec/cm
100 psi/cm

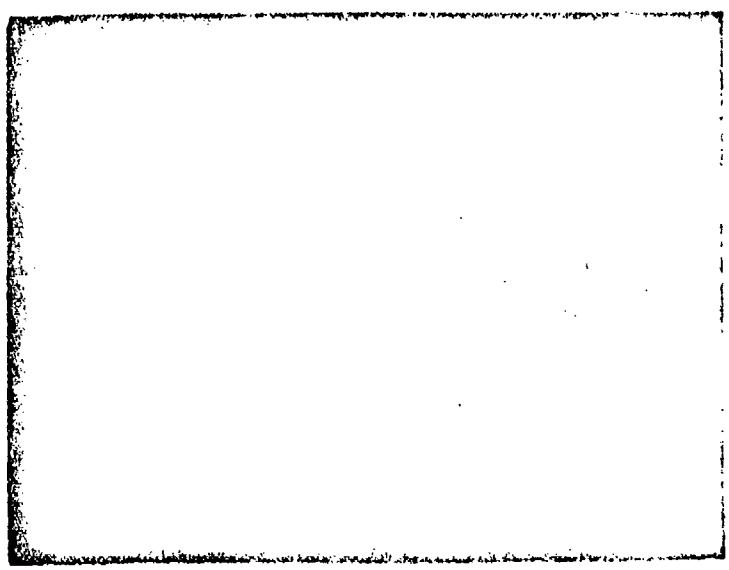

Gages 5 & 6, 0.5 msec/cm
100 psi/cm

Projectile velocity-
2830 fps

Figure 32
Scope picture, Series 2, Part 1, Shot 5A

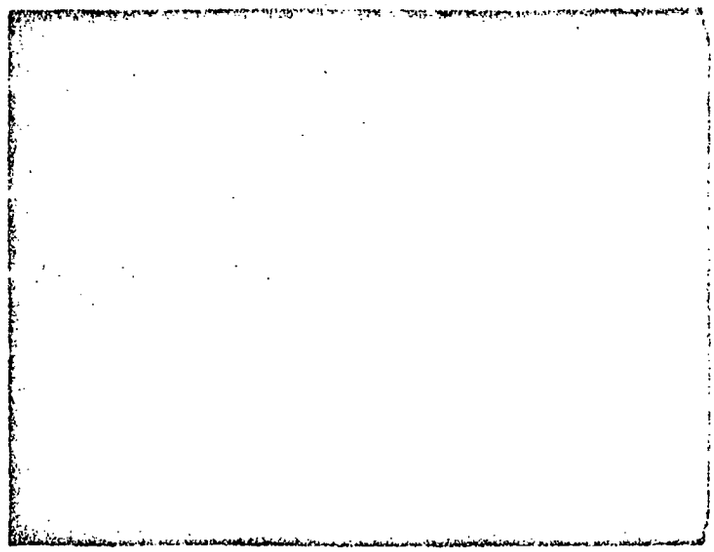

Shot 6A

Pneumacel

Gages 1 & 2, 2 msec/cm
200 psi/cm

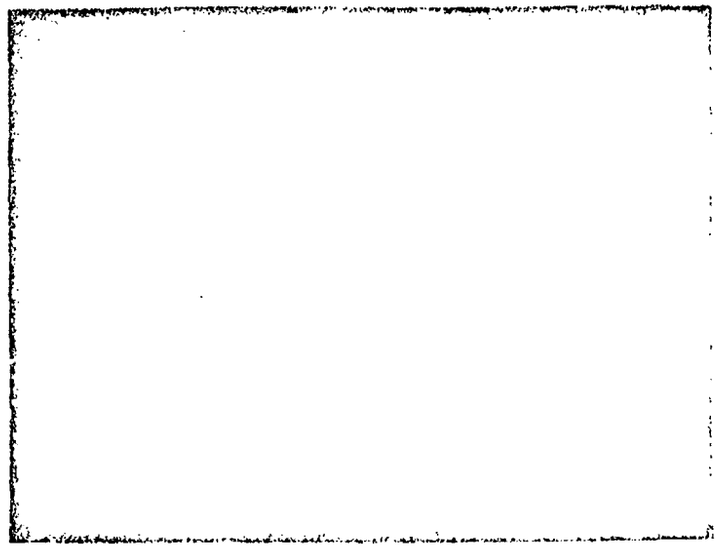

Gage 3, 0.5 msec/cm
400 psi/cm

Gage 4, 0.5 msec/cm
200 psi/cm

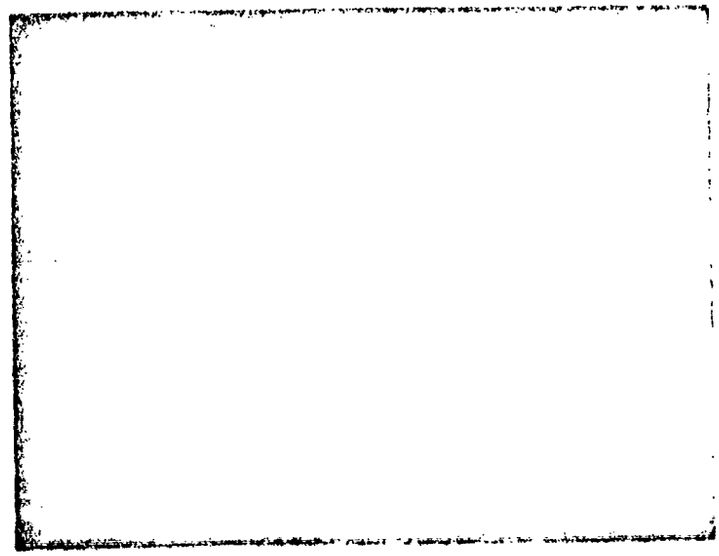

Gage 5, 0.5 msec/cm
200 psi/cm

Gage 6, 0.5 msec/cm
400 psi/cm

Projectile velocity-
2680 fps

Figure 33
Scope picture, Series 2, Part 2, Shot 6A

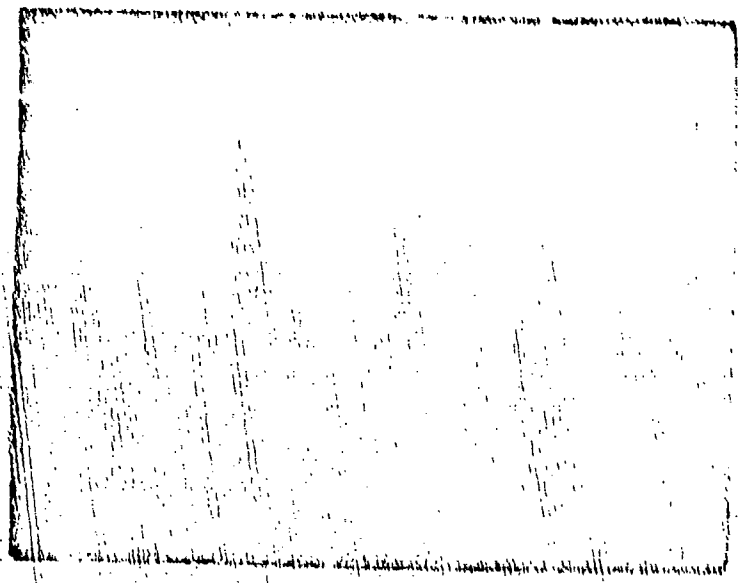

Shot 7A

Pneumacel

Gages 1 & 2, 2 msec/cm
200 psi/cm

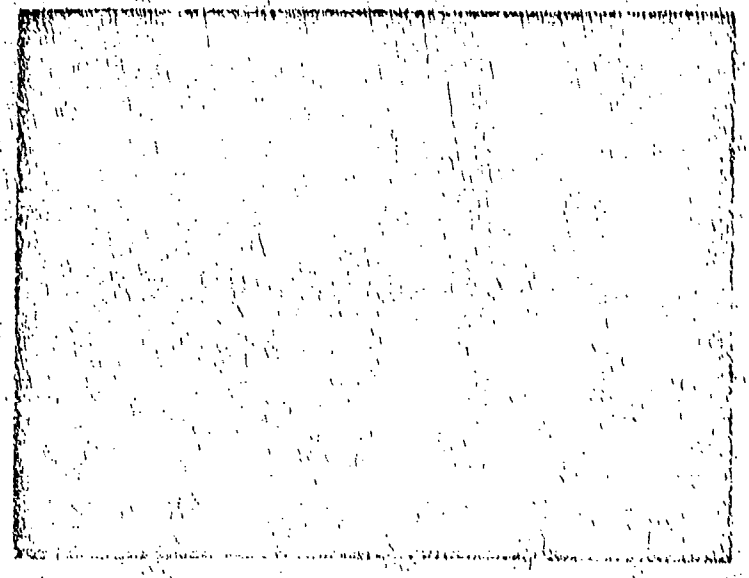

Gage 3, 0.5 msec/cm
400 psi/cm

Gage 4, 0.5 msec/cm
200 psi/cm

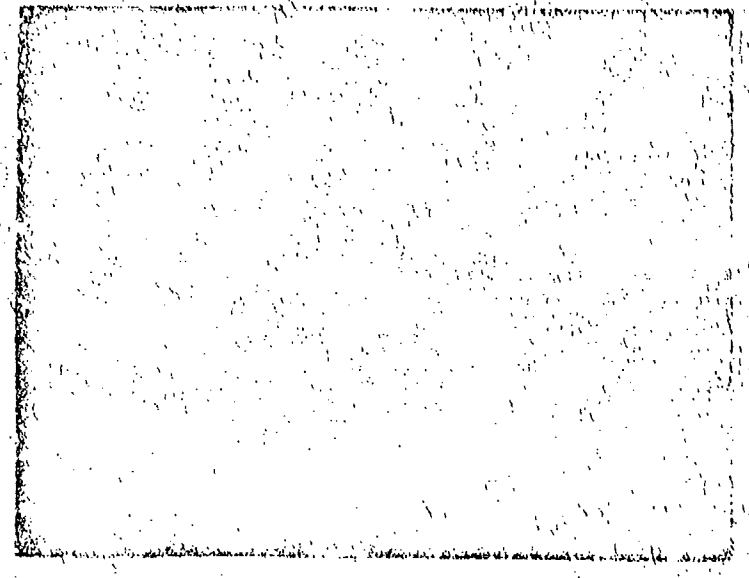

Gage 5, 0.5 msec/cm
200 psi/cm

Gage 6, 0.5 msec/cm
400 psi/cm

Projectile velocity-
2650 fps

Figure 34
Scope picture, Series 2, Part 2, Shot 7A

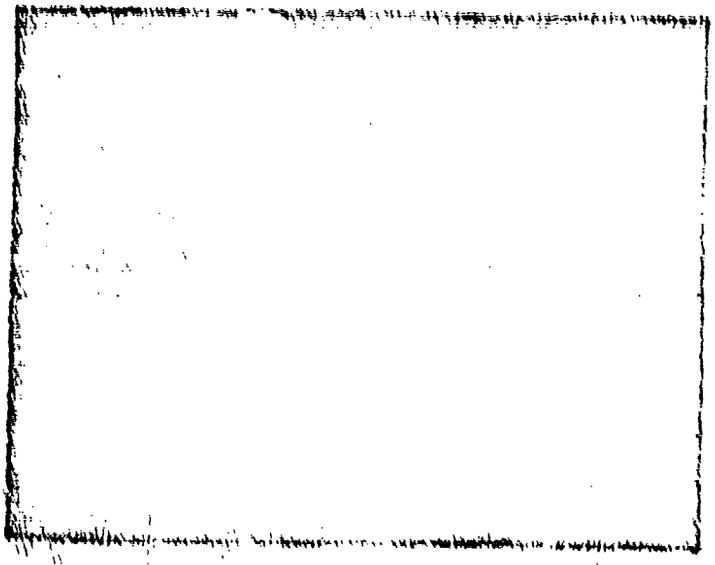

Shot 8A

Pneumocel

Gages 1 & 2, 2 msec/cm
200 psi/cm

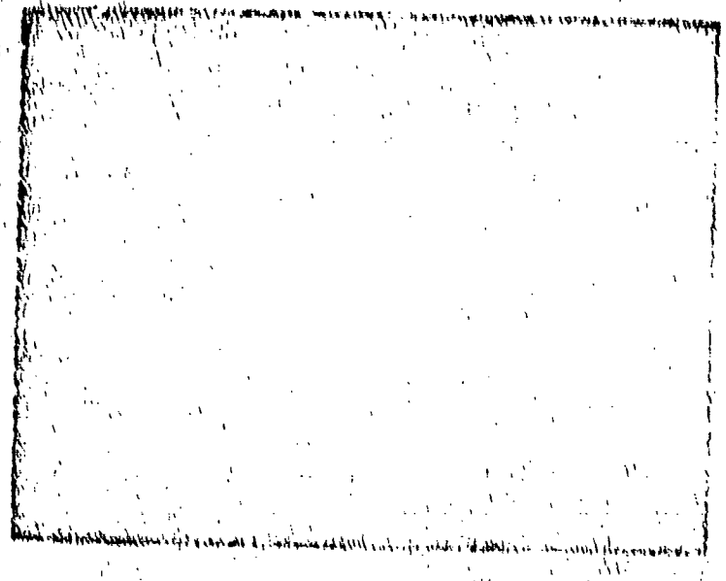

Gage 3, 0.5 msec/cm
200 psi/cm

Gage 4, 0.5 msec/cm
200 psi/cm

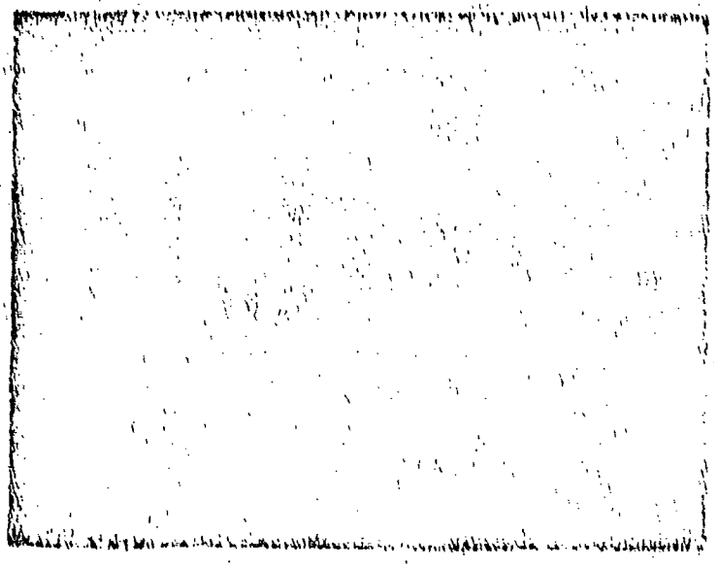

Gage 5, 0.5 msec/cm
200 psi/cm

Gage 6, 0.5 msec/cm
200 psi/cm

Projectile velocity-
2645 fps.

Figure 35
Scope picture, Series 2, Part 2, Shot 8A

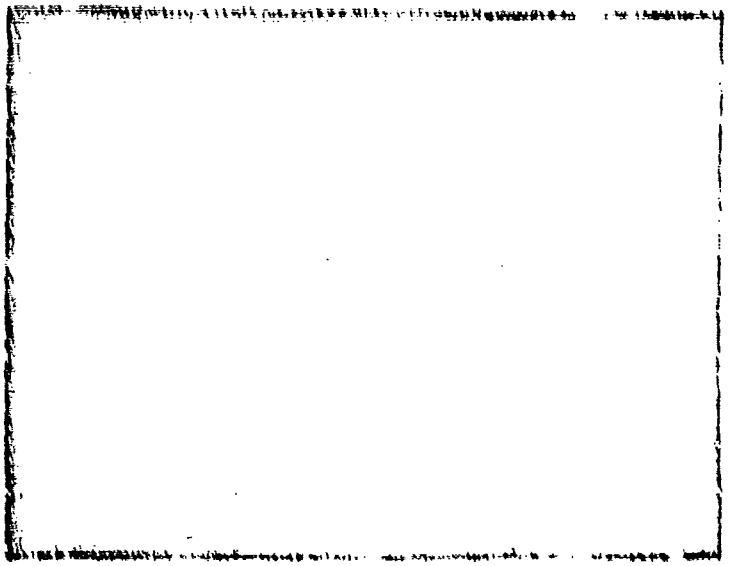

Shot 9A

Pneumacel

Gages 1 & 2, 2 msec/cm
200 psi/cm

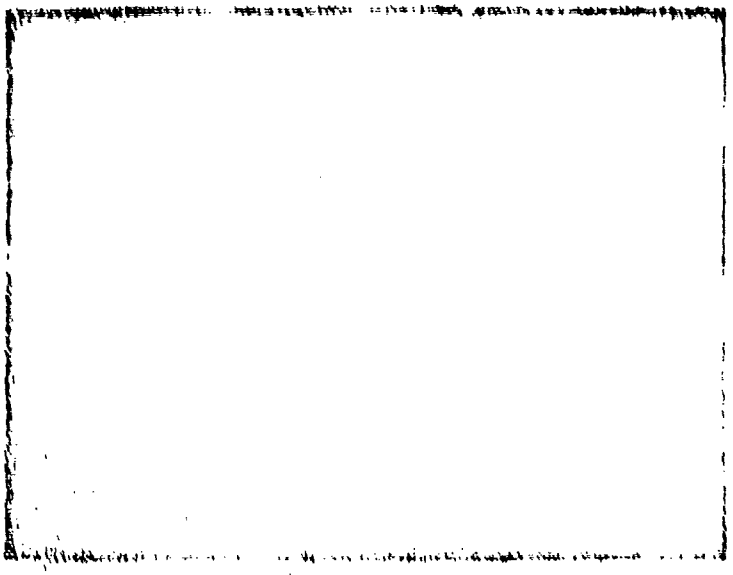

Gage 3, 0.5 msec/cm
400 psi/cm

Gage 4, 0.5 msec/cm
200 psi/cm

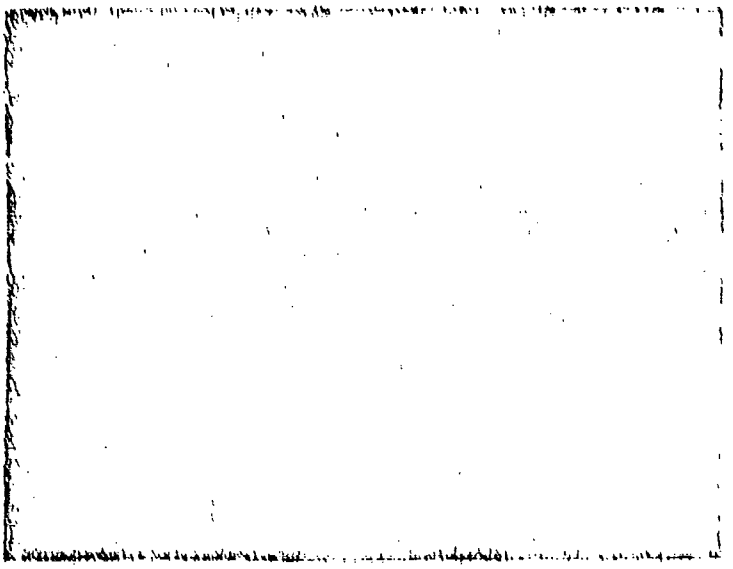

Gage 5, 0.5 msec/cm
200 psi/cm

Gage 6, 0.5 msec/cm
400 psi/cm

Projectile velocity-
2538 fps

Figure 36
Scope picture, Series 2, Part 2, Shot 9A

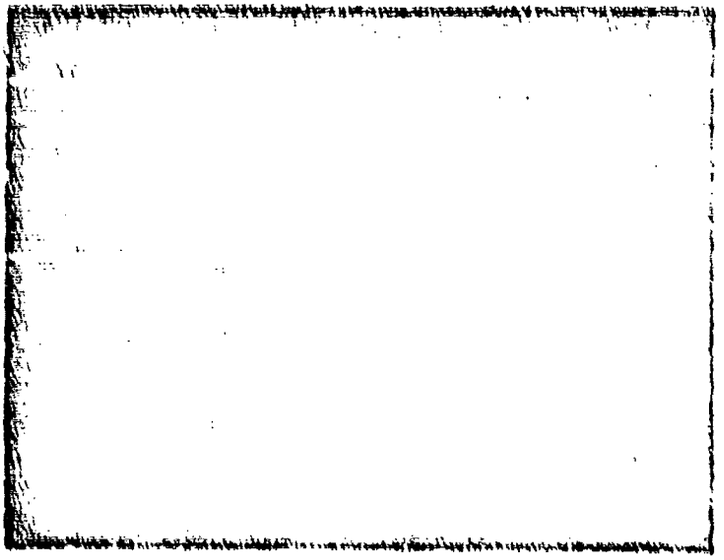

Shot 10A

Pneumagel

Gages 1 & 2, 2 msec/cm
200 psi/cm

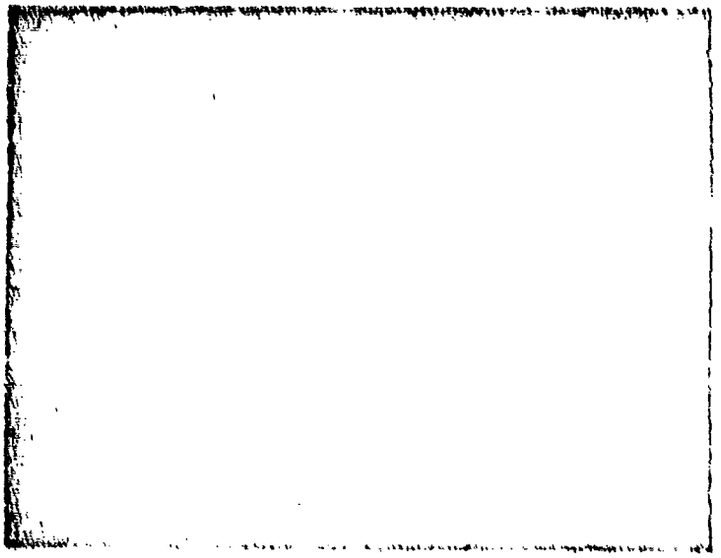

Gages 3 & 4, NO DATA

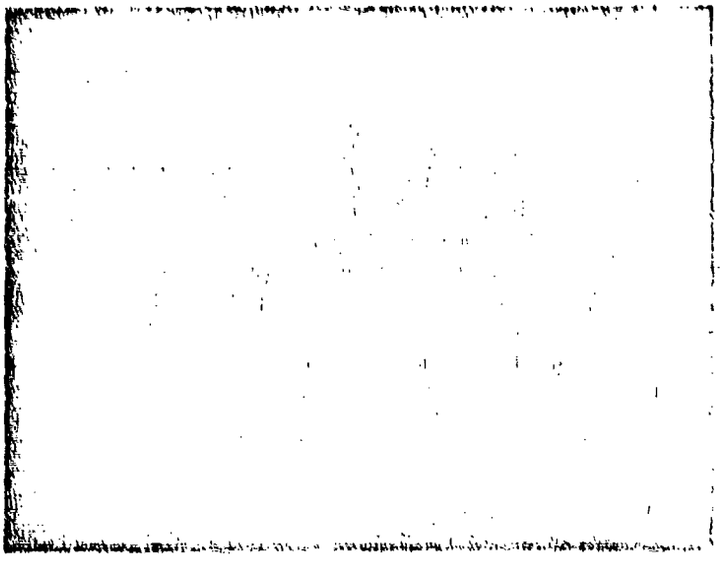

Gage 5, 0.5 msec/cm
200 psi/cm

Gage 6, 0.5 msec/cm
400 psi/cm

Projectile velocity-
2688 fps

Figure 37
Scope picture, Series 2, Part 2, Shot 10A

Vita

John R. Breuninger, Jr. was born on 29 July 1944 in Holyoke, Mass. He graduated from high school in St. Petersburg, Fla. He received his Associates in Arts degree from St. Petersburg Jr. College, and received his B.S. in Aerospace Engineering from the University of Florida in 1967. He entered the Air Force in November 1967 and received his commission through OTS on 16 Feb 1968. He served as a Project Officer for the Aerial Recovery Office at SAMSO in Los Angeles, Calif. from 1968-1971. In June 1971 he entered the Graduate Astronautical Engineering program at the Air Force Institute of Technology School of Engineering.

Permanent Address:

7225 Lynnwood Avenue N.
St. Petersburg, Florida

This thesis was typed by Mrs. Carmma Troxell